CHAPTER-1

INTRODUCTION

1.1 Introduction

This investigation documents the aerodynamic characteristics of four profiles, as cylinder, sphere, symmetrical aerofoil (NACA 0015) and cambered aerofoil (NACA 4415) objects of same volume. These have been analyzed in a comparison study dealing with their aerodynamic properties, tested at a sub-sonic wind tunnel and obtained experimental data at different Reynolds's Number and angle of attack. Improvement of our understanding of aerodynamic drag force experienced by the different shape of objects, are important for the design strategies of turbine blades, aerodynamic body, aero plane, high architectural structure etc. This performance dataset may be helpful in validating aerodynamic force prediction codes in support of such design activities.

1.2 Principle of Lift and Drag

The flow of air through the surfaces of aerodynamic shapes produces the lifting force and Drag forces. The two primary aerodynamic forces at work in aerodynamic shapes are lift, which acts perpendicular to the direction of wind flow and drag, which acts parallel to the direction of wind flow.

The angle between the relative wind and the chord line is the angle of attack of the airfoil. The lift and drag forces developed by an aerofoil will vary with the change of *angle of attack*. The drag forces of spherical and cylindrical shape at different angles should be similar. The slight difference occurs due to the surface unevenness and dissimilitude of shape.

The aerodynamic characteristics are strongly affected by the shape of the wing or blades section. The cross-sectional shape obtained by the intersection of the wing with the perpendicular plane is called an aerofoil. Here NACA 0015 and NACA 4415 symmetric aerofoil profiles have been used for the present research work. The lift force increases almost linearly with angle of attack until a maximum value is reached where upon the aerofoil is said to stall. The shape of the drag force vs. angle of attack is approximately parabolic. It is desirable for the wing to have the maximum lift and smallest possible drag.

The variation of lift and drag forces with angle of attack for a typical aircraft are shown in **Figure 1.1:**

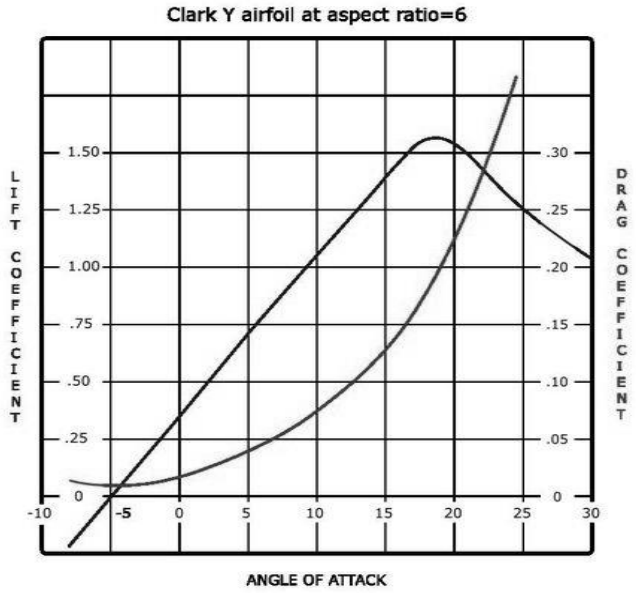

Figure 1.1: Variation of Lift and Drag Forces with Angle of Attack for a Typical Aircraft of Symmetric Aerofoil [1].

1.3 Boundary Layer

Fluid mechanics, a boundary layer is the layer of fluid in the immediate vicinity of a bounding surface where the effects of viscosity are significant. Aerodynamic forces depend in a complex way on the viscosity of the fluid. The details of the flow within the boundary layer are very important for many problems in aerodynamics, including wing stall, the skin friction drag on an object, and the heat transfer that occurs in high speed flight.

Boundary layers may be either laminar (layered), or turbulent (disordered) depending on the value of the Reynolds number. For lower Reynolds numbers, the boundary layer is laminar and the stream wise velocity changes uniformly as one moves away from the wall, as shown on the left side of the **Figure 1.2**. For higher Reynolds's numbers, the boundary layer is turbulent and the stream wise velocity is characterized by unsteady swirling flows inside the boundary layer.

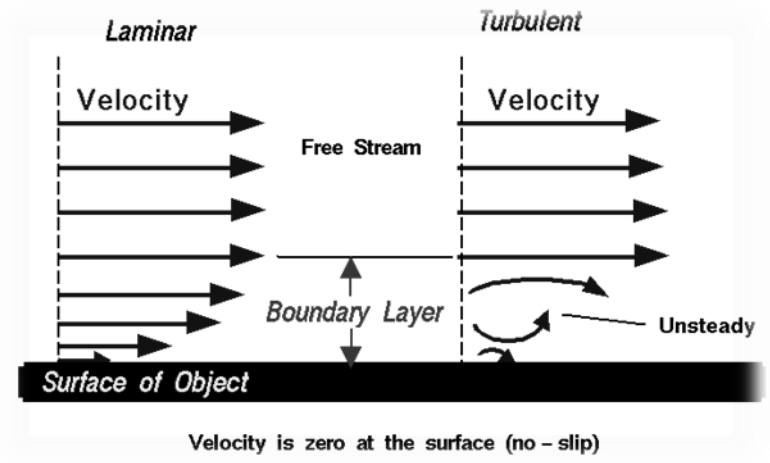

Figure 1.2: Laminar and Turbulent Flow of Boundary Layers.

1.4 Objective with Specific Aims and Possible Outcome

The 1st objective of this experiment was analyzing the performance of all the profiles at different Reynolds's Number. The profiles are spherical ball, cylindrical solid shape, symmetric aerofoil (NACA 0015), cambered aerofoil (NACA 4415) of same volume.

The 2nd objective is to obtain experimental data at different Reynolds's Number and angle of attack. The two aerofoils (symmetrical NACA 0015 and cambered NACA 4415) have been tested from -3˚ to 21˚ angles of attack with 3˚ steps and spherical ball, cylindrical shaped profiles have been tested from at 0˚ to 180˚ angles with 10˚ steps at different Reynolds Number.

1.5 History and Background

In both Aerospace and Automotive industry, aerodynamics plays a critical role in vehicle design. Shapes and designs are optimized to obtain the lowest drag possible. One way of expressing drag is by using drag coefficients. The drag coefficient is a dimensionless number used to represent the overall effects of shape, inclination, and other flow conditions.

The earliest serious work on the development of airfoil sections began in the late 1800's. H.F. Phillips patented a series of airfoil shapes in 1884 after testing them in

one of the earliest wind tunnels [2]. At nearly the same time Otto Lilienthal had similar ideas. He believed that the key to successful flight was wing curvature or camber. Wright Brothers closely resembled the aerofoil of Lilienthal's sections which are thin and highly cambered. Probably early tests of airfoil sections were done at extremely low Reynolds number, where such sections behave much better than thicker ones.

A wide range of airfoils were developed, based primarily on trial and error. Some of the more successful sections such as the Clark Y and Gottingen 398 were used as the basis for a family of sections tested by the NACA in the early 1920's.

In 1939, Eastman Jacobs at the NACA in Langley, designed and tested the first laminar flow airfoil sections. These shapes had extremely low drag and the section shown here achieved a lift to drag ratio of about 300.

CHAPTER-2

LITERATURE REVIEW

2.1 Aerodynamic Forces Experienced by an Aircraft

Aerodynamic forces are experienced when an aerofoil placed in the uniform flow of an air stream which is created by virtue of the relative motion. The resultant of these aerodynamic forces can be resolved into two force components, parallel and perpendicular to the main flow direction. The vertical force exerted by the fluid on the body is termed as *lift* force, and the component of the total aerodynamics reaction which is parallel and opposite to the flight path of aircraft is called the *drag* force. Among the drag forces, surface friction drag and form drag are called parasite drag and induced drag or vortex drag and increment of zero lift drag are called induced drag.

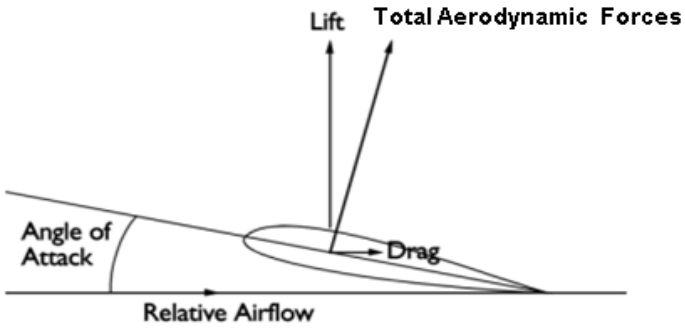

Figure 2.1: Aerodynamic Forces on a Typical Aerofoil

Lift and drag force data are usually expressed in dimensionless terms by using **lift coefficient** and **drag coefficient**. The lift coefficient is defined as:

$$C_L = \frac{L}{\frac{1}{2}\rho V^2 S.}$$

Here, L is the Lift produced, ρ is the Density of air, V is the Velocity of the body and S is the Area of the body or aerofoil. Again, the drag coefficient is defined as:

$$C_D = \frac{D}{\frac{1}{2}\rho V^2 S.}$$; Where D id the drag force.

2.2 Lift and Drag of a Circular Cylinder

The lift generated by an airplane wing or a curving baseball is quite familiar. A simple rotating cylinder also creates lift. Kutta-Joukowski lift theorem for a cylinder is used to explain the situation.

The basic assumption on which the analysis is founded is that air is an inviscid fluid. It is necessary to recognize that the viscosity, though very small, is non-zero, but this will have little effect on the magnitude of the result coated. Another assumption of the theory as presented here is that the flow is two dimensional. So, there is thus only two degree of freedom.

The circular theory is applied in circular cylinder. First consideration is, Circular Cylinder without Circulation, therefore, the flow past an infinite circular cylinder placed in a uniform stream of air, without circulation. The streamline pattern which results is depicted in **Figure 2.2.**

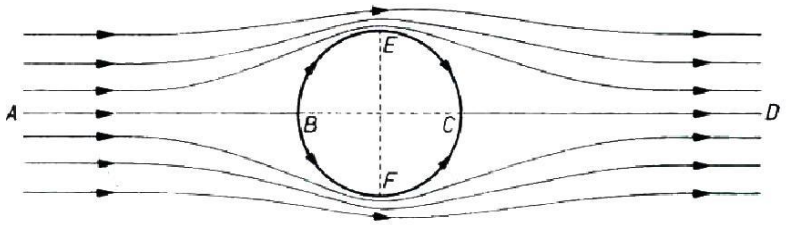

Figure.2.2: Circular Cylinder without Circulation

The line ABCD is a dividing streamline, which separates the fluid which passes over the top of the cylinder from that which passes bellow it. The points B and C are stagnation points. The fact should be noted that, the doubly symmetric streamlines are close together near the top with high velocity and bottom of the cylinder are far apart near the front and rear having low velocity. As streamline is doubly symmetric so the velocity distribution, hence, by Bernoulli's Theorem, the pressure distribution, are also doubly symmetric. The stagnation points are also symmetrically located at opposite end of the horizontal diameter. It follows that there is no lift and no drag.

Now the consideration is a circular cylinder with Circulation in a uniform stream, with circulation r (a free vortex of that strength) superimposed. The circulation is in clockwise direction. The streamline pattern is then as depicted in **Figure 2.3**;

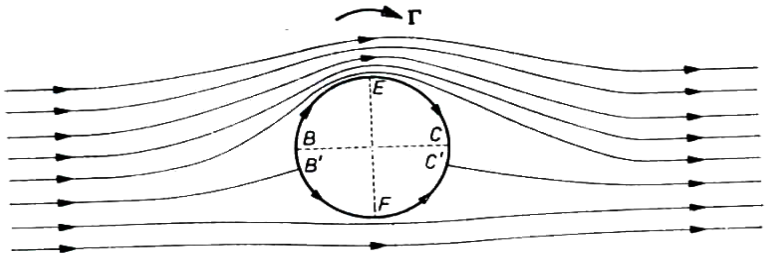

Figure 2.3: A circular cylinder with Circulation**.**

The total velocity at B is in upward sense above the dividing streamline, as must C. There are two points Ḃ and Ċ, below B and C, therefore the new stagnation point, the effect of superimposing the circulation on the original flow are, the amount of downward movement of stagnation points depends on the magnitude of the circulation in relation to the free stream speed. The circulation also increases the speed over the upper surface and reduces the speed over the lower surface of the cylinder. From the Bernoulli's Theorem, therefore, it follows that the pressure is generally reduced on the upper surface and increase on the lower surface. So the net force vertically upwards is lift. The streamline pattern is still symmetrical about the diameter EF (Figure 2.3). It follows that there is still no drag. [1]

Drag force varies with Reynolds number. Theoretically in subsonic level of air speed the curve is a straight line in the **Figure 2.4** [(Scruton and Rogers, 1971). As the investigation is done at 10 m/s to 25 m/s air speed, so in this range the graph shows a straight line.

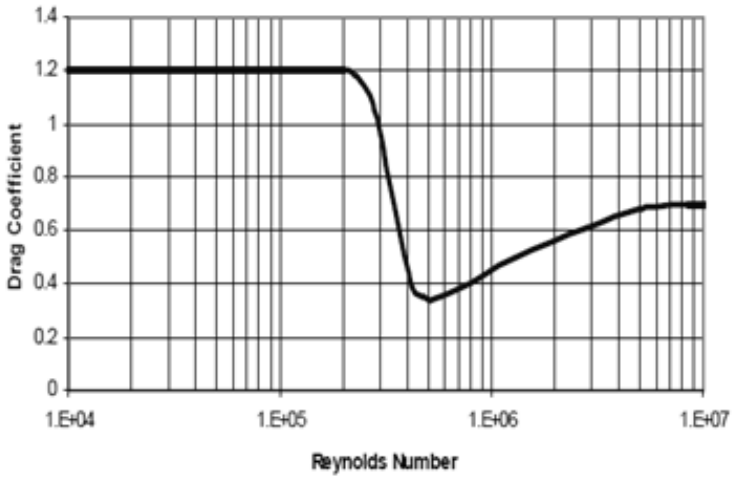

Figure 2.4: Drag Coefficient vs. R_e number for a circular cylinder (Scruton and Rogers, 1971).

2.3 Lift and Drag of a Sphere

Necessity of Creation of lift is to turn a flow of air. Where there is less amount of drag, more lift is produced. The airfoil of a wing turns a flow, and so does a rotating cylinder. A spinning ball or sphere also turns a flow and generates an aerodynamic lift and drag force.

Next to any surface, the molecules of the air stick to the surface, as discussed in the properties of air slide. This thin layer of molecules entrains or pulls the surrounding flow of air. For a spinning ball the external flow is pulled in the direction of the spin. If the ball is translating through the air at some velocity, then on one side of the ball the entrained flow opposes the free stream flow, while on the other side of the ball, the entrained and free stream flows are in the same direction. The flow is then turned by the spinning ball, and a force is generated. Because of the change to the velocity field, the pressure field is also altered around the ball [5].

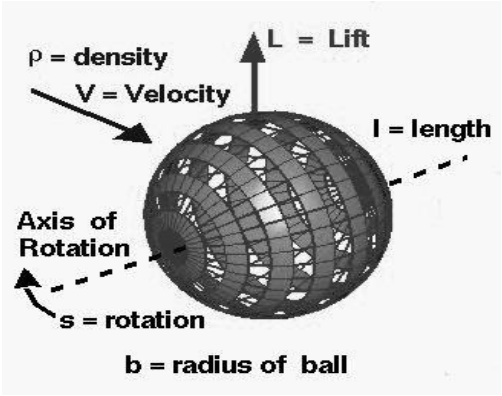

Figure 2.5: A circular sphere.

The variation of drag coefficient with Reynolds number is seen in the **Figure 2.6**. The curve is a parabolic curve in ideal case.

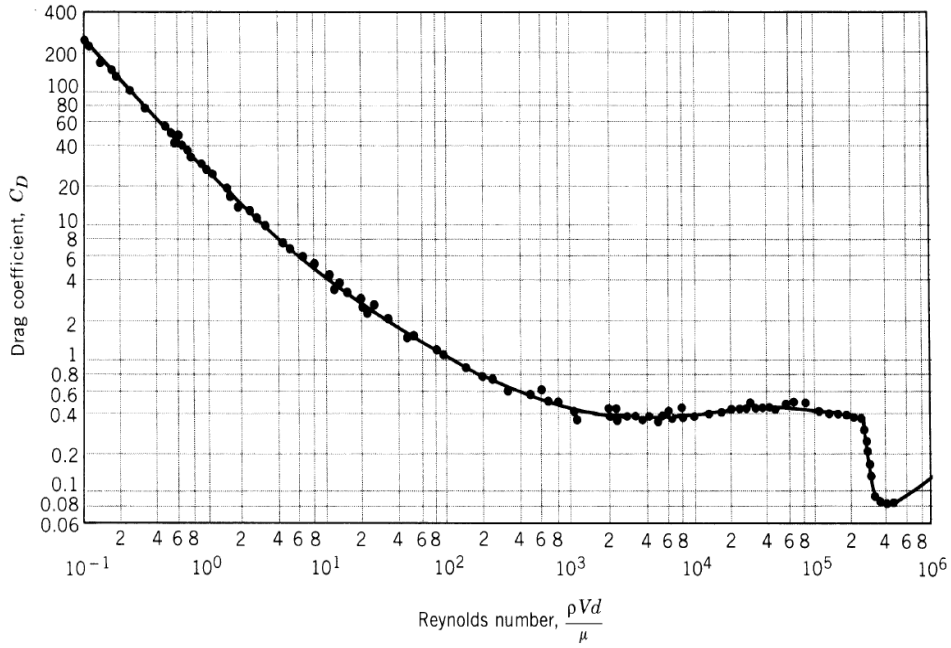

Figure 2.6: Variation of drag coefficient with Reynolds number for a sphere in ideal case [6].

If a cylinder or sphere with roughed surface in a stream of air is rotating, the rough surface of the cylinder, through friction, causes the air in the vicinity to travel round with it, thus inducing circulation, which gives rise to lift. This phenomenon is known as the Magnus effect. For example this effect is responsible for the swing of a sliced golf tennis ball.

2.4 Flows past a Two-dimensional Aerofoil

The study of flow of air is very important for aerodynamic application. The stream line flow pattern is also a useful aid in study of aerodynamics. Considering, a flow of air over an aerofoil. Both the air speed and direction over the aerofoil can vary from point to point. The path followed by the moving fluid element is called a streamline of the flow. The motion of the air over the aerofoil can be easily visualized by drawing the streamlines of the actual flow field. The figure shows the streamline over an aerofoil.

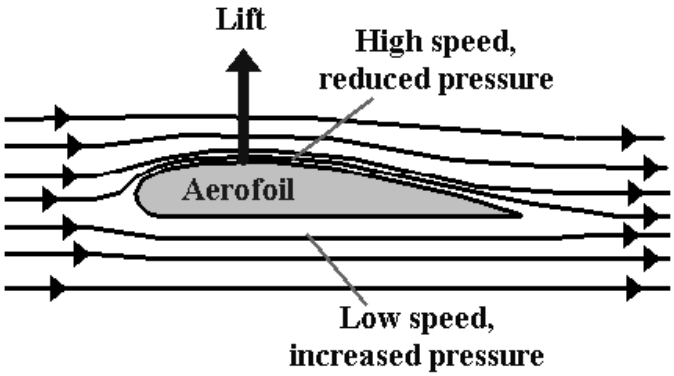

Figure 2.7: Two-dimensional Aerofoil

Considering, the flow of air over the surface of a body, with a strong adverse pressure gradient, i.e. pressure increasing rapidly in the stream direction**.** The particles of fluid in the relatively slowly moving region near the surface of the body will be retarded by this pressure forces. If the pressure gradient is strong enough, the velocity near the surface will fall to zero, and subsequently be reverse in direction. If this occurs large eddies will form and the streamline will lifted well away from the surface, creating a large region of slowly moving, eddying flow known as the dead air region (**Figure 2.8**). This is the phenomenon of separation.

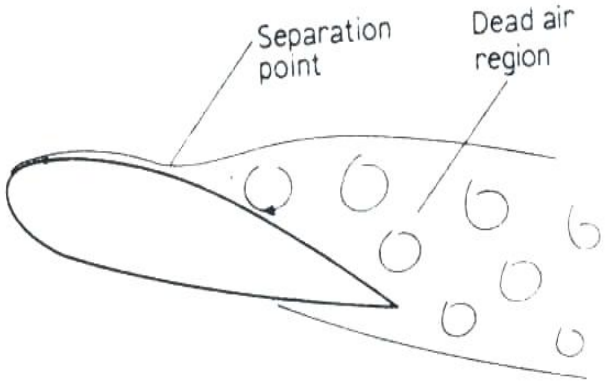

Figure 2.8: Air flow separation from aerofoil section.

The effects of flow separation are breakdown of streamline flow with a sudden reduction of the lift and increase in form drag of the body. There is also a sudden destruction of the adverse pressure gradient which caused the flow reversal in the first place. The unsteadiness in the flow also results buffering of the body [1].

2.4.1 Aerofoil Terminology

The cross-sectional shape obtained by the intersection of an aircraft wing with the perpendicular plane is called an aerofoil [Anderson 1991 and Glauert 1926]. The major design feature of an aerofoil is the mean camber line. Mean Camber Line is the line drawn halfway between upper and lower surfaces. The most forward and rearward points of the mean camber line are the leading and trailing edges respectively. Straight line connecting leading edge and trailing edge is called Chord Line of an aerofoil and length of chord line in the aerofoil is called Chord Length. Maximum distance between mean camber line and chord line is Maximum Camber and Maximum Thickness is the distance between upper and lower surfaces of an aerofoil. The most significant terminology of aerofoil is the angle of attack. It is the angle between the wing chord line and the direction of the flight path. Lift and drag of an aircraft mainly depends on it.

The measure of sharpness of leading edge of aerofoil is the Leading edge radius. And the aspect ratio of a wing is the span (b) divided by the geometric mean chord (c). Thus, AR = b/c = b^2/bc = b^2/S.

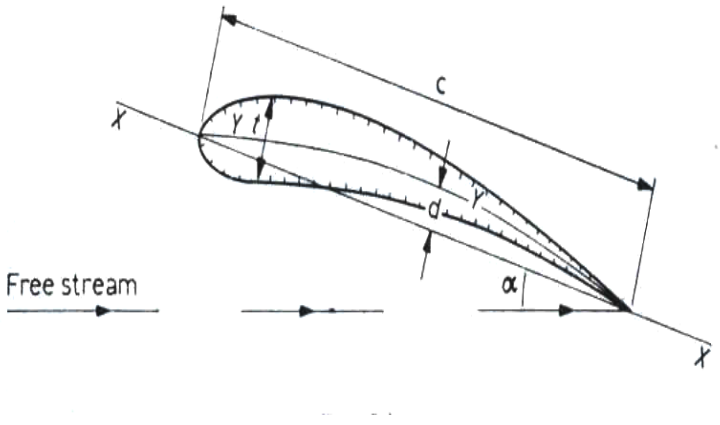

Figure 2.9: Aerofoil Terminology

Here, ‘XX’ is the Chord Line, ‘c’ means Chord Length, ‘t’ is the Max Thickness, ‘YY’ indicates the Camber Line, ‘α’ specifies the Angle of Attack and ‘d’ is called the Max Camber.

There are various types of aerofoil like 4-digit, 5-digit, modified 4-/5-digit, 6-digit etc. There were many similarities between those airfoils but mainly two primary variables affect the shapes of an aerofoil which are the slope of the airfoil mean camber line and the thickness distribution above and below this line. These variations lead a series of equations to generate an entire family of related NACA airfoil shapes. 4-digit NACA 0015 symmetrical aerofoil profile and cambered aerofoil NACA 4415 of same volume have been chosen in this research work. The explanation of the 4-digit NACA 0015 and NACA 4415 aerofoil is as follows:

a. The first digit specifies the maximum camber in percentage of the chord [Abbott and Albert 1945 and 1959],

b. The second digit indicates the position of the maximum camber in tenths of chord [Abbott and Albert 1945 and 1959] and

c. The last two digits provide the maximum thickness of the airfoil in percentage of chord [Abbott and Albert 1945 and 1959].

The thickness distribution above (+) and below (-) the mean line can be calculated by the following equation for each of the x-coordinates of 4-digit NACA symmetrical aerofoil [Abbott and Albert 1959]:

The Drag coefficient also varies for NACA 0015 symmetrical aerofoil and NACA 4415 cambered aerofoil. From the Figure 2.10 for NACA 0015 symmetrical aerofoil, it is seen that the drag coefficient starts to increase rapidly after 14˚-15˚ AOA whereas for NACA 4415 cambered aerofoil, the drag coefficient increased rapidly at 16˚-18˚ AOA in **Figure** 2.11.

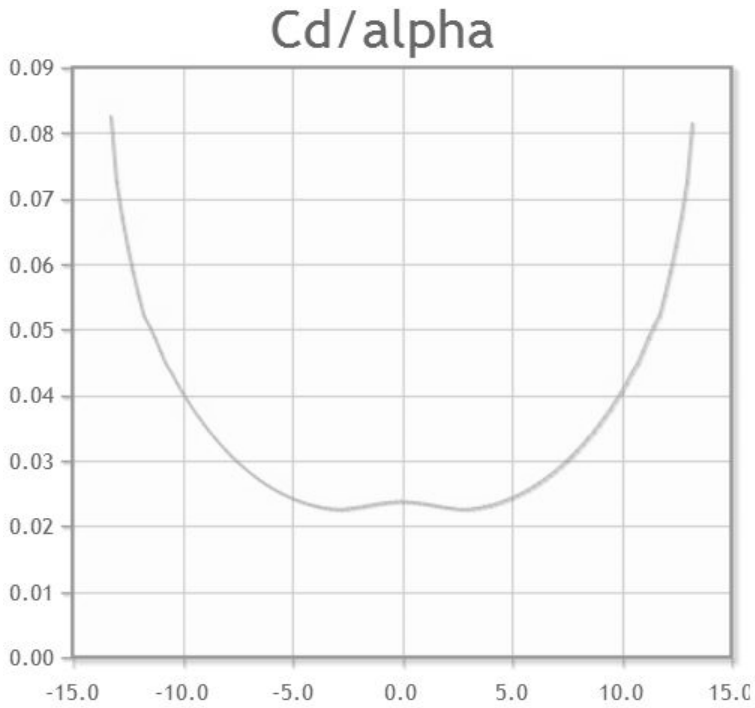

Figure 2.10: The Drag coefficient vs. Angle of Attack graph of NACA 0015 symmetrical aerofoil [7].

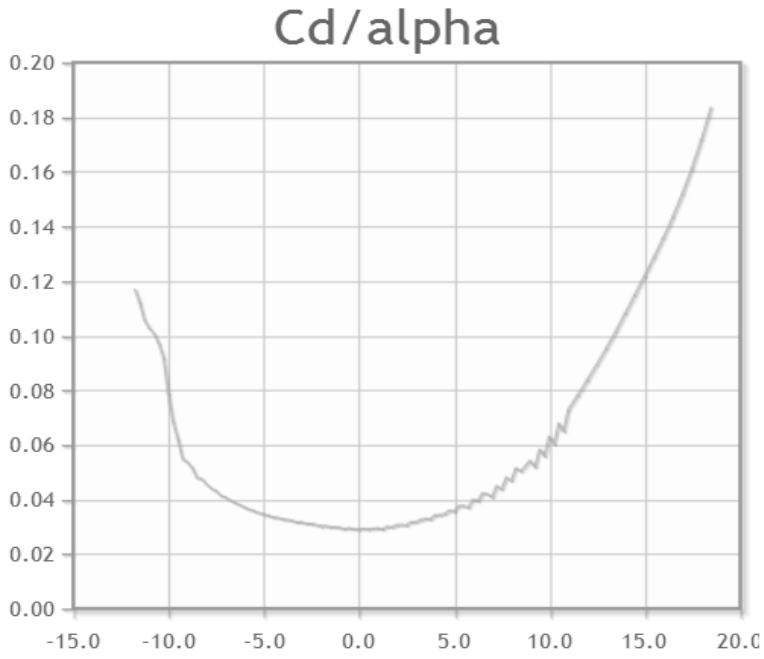

Figure 2.11: The Drag coefficient vs. Angle of Attack graph of NACA 4415 cambered aerofoil [8].

CHAPTER-3

EXPERIMENTAL SETUP

3.1 Wind Tunnel AF 100

A wind tunnel is test bench used in aerodynamic research to study the effects of air moving past solid objects. AF100 is a compact, practical open circuit suction wind tunnel for studying aerodynamic. Air enters the tunnel through an aerodynamically designed effuse that accelerate the air linearly to the working section, passes through a grill, a diffuser and then to a variable speed axial fan. The air leaves the fan, going through a silencer unit to the atmosphere. The test object is instrumented with a sensitive balance to measure the forces generated by airflow.

Wind tunnel AF 100 is an open circuit subsonic wind tunnel for a wide range of investigation in to aerodynamics with a working section of 300 mm by 300 mm and 600 mm long. The forces of three component balance, electronic sensors on the optional wind tunnel instrumentations are connected to Versatile Data Acquisition System (VDAS).

Figure 3.1: Wind Tunnel AF 100.

3.1.1 Major Parts:

3.1.1.1 Effuser (Contraction Cone) - The Effuser accelerates the airflow linearly. A Large volume of low velocity air is converted into to a small volume of high velocity air without creating turbulence.

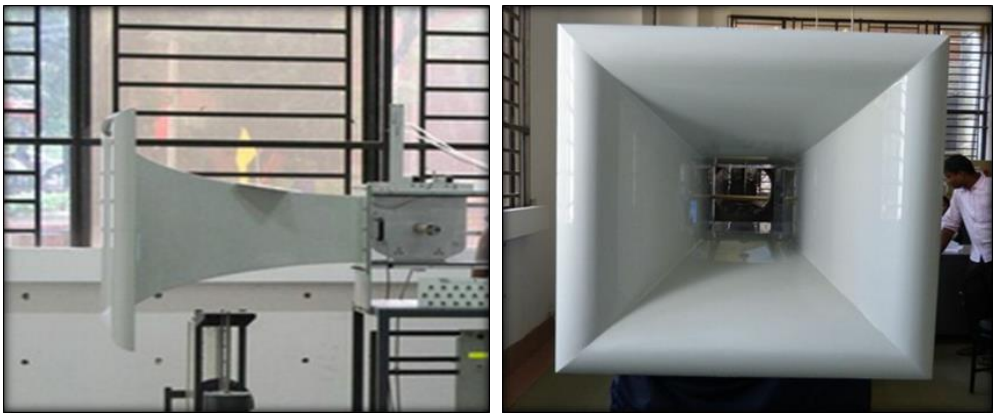

Figure 3.2 : Effuse or Contraction Cone (Side and Front View).

3.1.1.2 Working Section

The working section of the wind tunnel is a square section with a clear roof, sides and floor. The sides are removable. A pitot static tube and a traversing pitot tube fit on the working section, upstream and downstream of any models.

Figure 3.3: Working Section of Wind Tunnel AF 100.

3.1.1.3 Three Component Balance (AF A3)

The working section has three component balance (AF A3) which measure the angular position of models mounted on the balance in TecQuipment's Subsonic Wind Tunnel (AF100). It provides convenient support system for

models to measure the lift, drag and pitching moment exerted on the model. To enable accurate real-time data capture, monitoring and display on a computer, a fully compatible TecQuipment's Versatile Data Acquisition System (VDAS) has been used. Digital display shows lift, drag and pitching moment directly. It also provides full adjustment of angle of incidence of the model to direction of air flow.

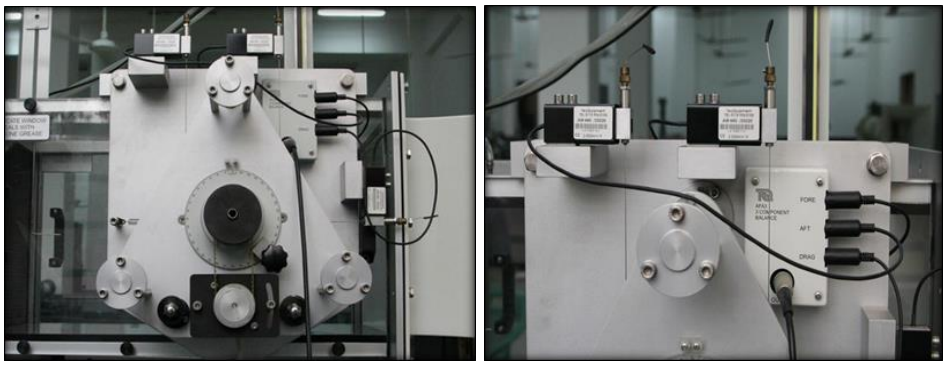

Figure 3.4: Three Component Balance.

3.1.1.4 Balance Angle Feedback Unit

The Balance Angle Feedback Unit is an optional ancillary for use with Three Component Balance (AFA3) to measure the angular position of models mounted on the balance in Subsonic Wind Tunnel (AF100). The Angle Feedback Unit mounts on the Three-Component Balance attached to the wind tunnel. It then transmits the rotational angle of the model to VDAS.

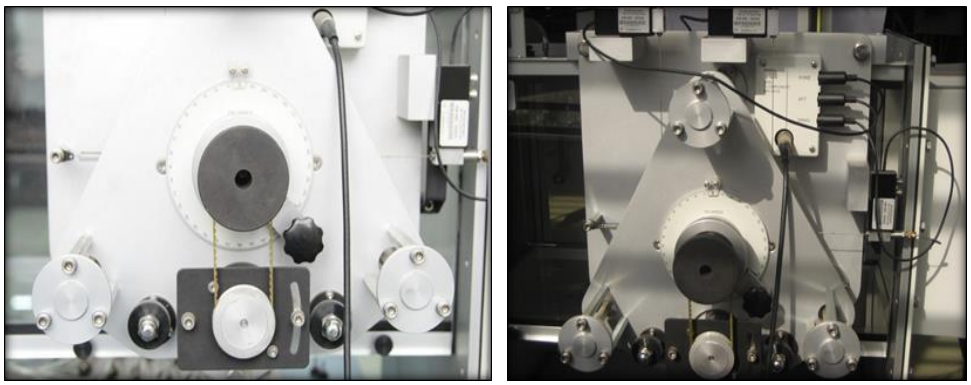

Figure 3.5: Balance Angle Feedback Unit

3.1.1.5 Diffuser and Fan

Diffuser slows the speed and brings steadiness in the air flow in the wind tunnel. Then the air flow out to a variable speed axial fan and through a silencer unit to the atmosphere.

Figure 3.6: Diffuser and Fan

3.1.2 Technical Data

ITEM	SPECIFICATION
Total length of apparatus	3700 mm
Total depth(front to back)	1065 mm
Total height	1900 mm
Working section	305 mmx305 mm x600 mm
Air velocity	0 to 36 m/s
Fan motor	AC three –phase axial variable speed
ELECTRICAL SUPPLY	
Type	Three phase AC
voltage(depend on demand)	415 V or 220 V
total current(with all optional instrument connected)	21A(415V)/26A(220V)
FUSES	
Drive unit	(415V)three phase 16AMCB(miniature circuit breakers)(220V)three phase 20A MCB
IEC outlets	10 A MCB
Low voltage instrumentation supply	2 A MCB

3.1.3 VERSATILE DATA ACQUISITION SYSTEM

VDAS is a highly accurate and effective tool with digital automatic data acquisition hardware, software and accessories. It's a Fast and automatic calculation, recording, charting, and exporting of relevant data and parameters. A computer interface units available in both frame mounting and bench top options. The computer enables real time data capture, recording, monitoring and display of all relevant parameters.

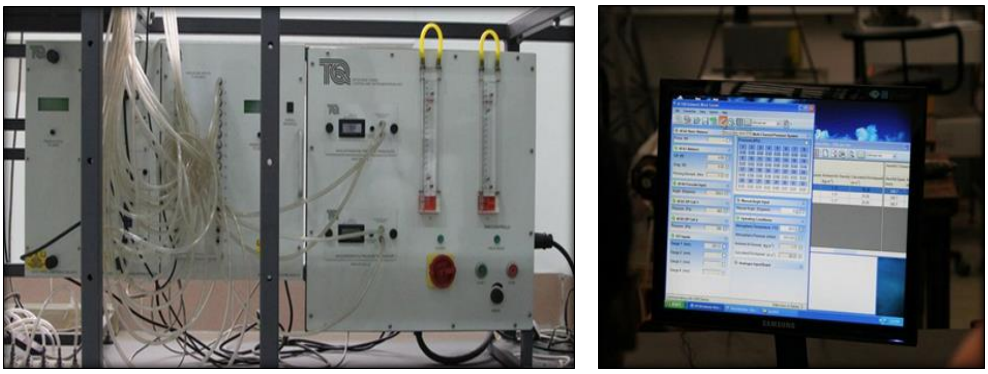

Figure 3.7: Versatile Data Acquisition System (VDAS).

3.2 Fabrication of the Profiles

Four different profiles, which are cylinder, sphere, symmetrical aerofoil (NACA 0015) and cambered aerofoil (NACA 4415), objects of same volume have been fabricated by the following processes.

- Construction profiles have been done by wood ('Gamary'). The four different are shown in the figure 3.7(a), 3.7(b), 3.7(c), 3.7(d).

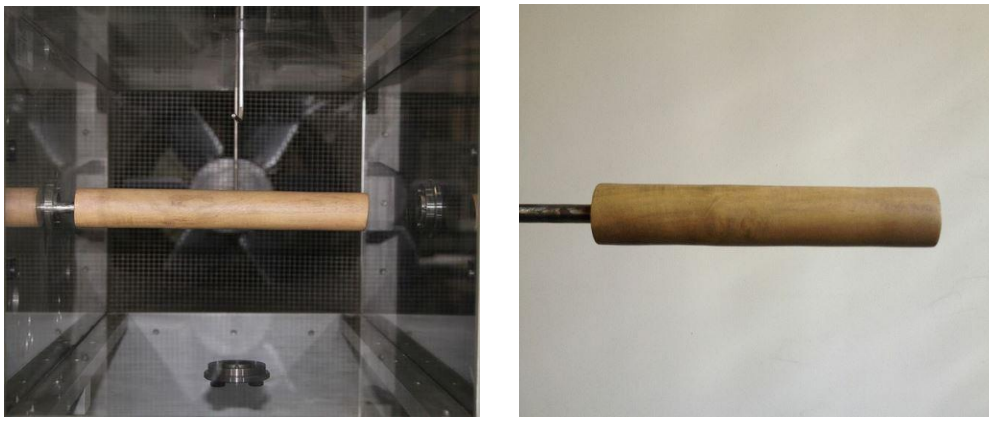

Figure 3.8(a): Cylindrical profile.


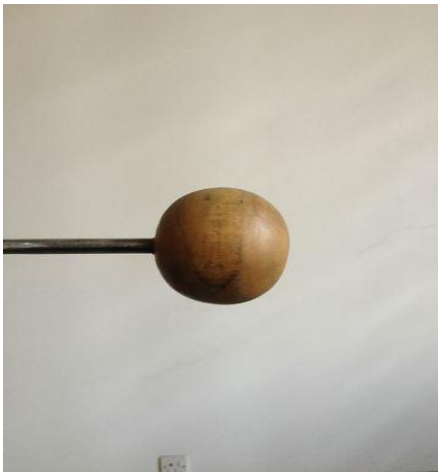

Figure 3.8(b): Sphere shaped profile.

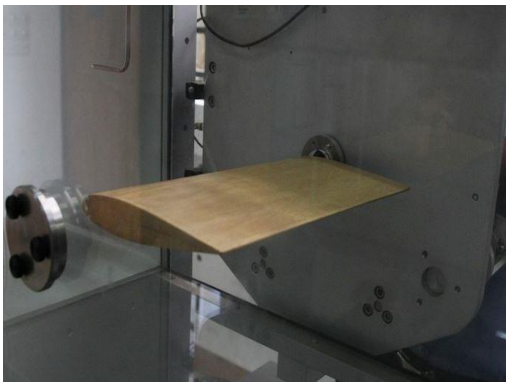
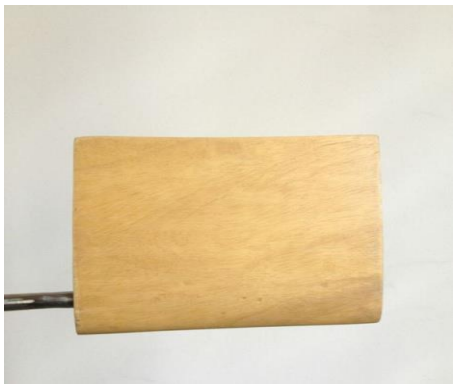

Figure 3.8(c): Symmetrical aerofoil (NACA 0015).

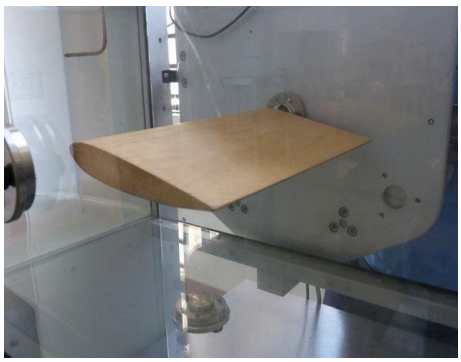


Figure 3.8(d): Cambered aerofoil (NACA 4415)

❖ The dimensions of the Profiles are:

a) The cylinder has diameter= 38.72 mm, length=247 mm.

b) The sphere has diameter= 90.8 mm.

c) The symmetrical aerofoil (NACA 0015) has chord length= 141.41mm and span=240.7 mm.

d) The cambered aerofoil (NACA 4415) has chord length=142.67 mm and span= 247 mm.

❖ The profiles have been hold in the working section of the wind tunnel AF100 with a hollow cylindrical steel rod. The dimensions of both the rods are: length= 20 cm, Diameter=12 mm. It is shown in Figure 3.8.

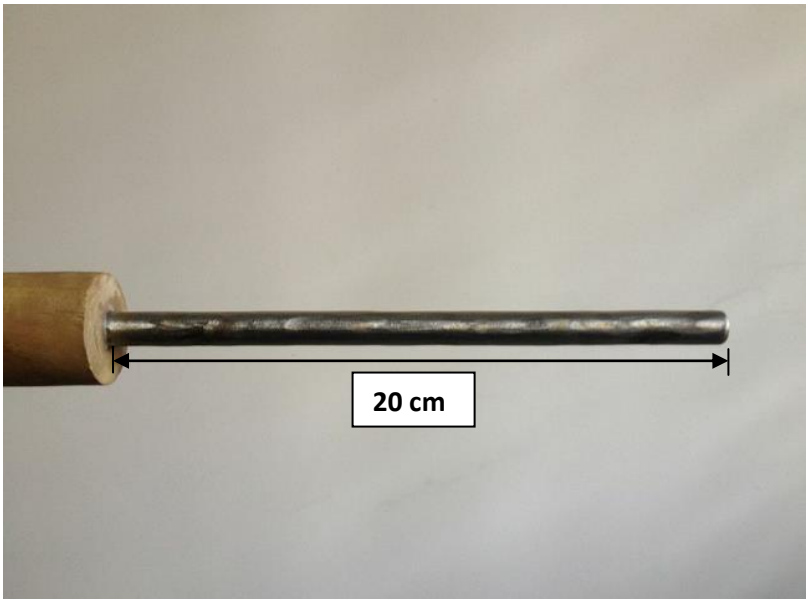

Figure 3.9: Hollow cylindrical steel rod attached with the profiles.

❖ The Cylindrical hollow rod has been attached to the profiles by drilling a hole with the drilling machine and inserting the rod into it. A polysynthetic resin adhesive has been given in the hole so that the rod couldn't move or come out.

Figure 3.10: Drilling of the profiles.

CHAPTER-4

EXPERIMENTAL RESULTS

4.1 Collection of Experimental Data

For investigation of the aerodynamic characteristics of four profiles, as cylinder, sphere, symmetrical aerofoil NACA 0015 and cambered aerofoil (NACA 4415) objects. Test has been conducted in subsonic wind tunnel AF100. The flow is considered to be incompressible and subsonic flow and the effect of temperature is neglected. The experimental data have been obtained at different Reynolds Number and angle of attack the two aero foils (symmetrical NACA 0015 and cambered NACA 4415) have been tested from -3˚ to 21˚ angles of attack with 3˚ steps and spherical ball, cylindrical shaped profiles have been tested from at 0˚ to 180˚ angles with 10˚ steps at different Reynolds Number.

4.2 Aerodynamic Characteristics of NACA 0015

The variation of drag coefficient with Reynolds number for symmetric aerofoil NACA 0015 is shown in following **Figure 4.1** to **Figure 4.9**. The drag coefficient simultaneously decreases and gives a downward curve with the increase of Reynolds number of the air for each angle of attack.

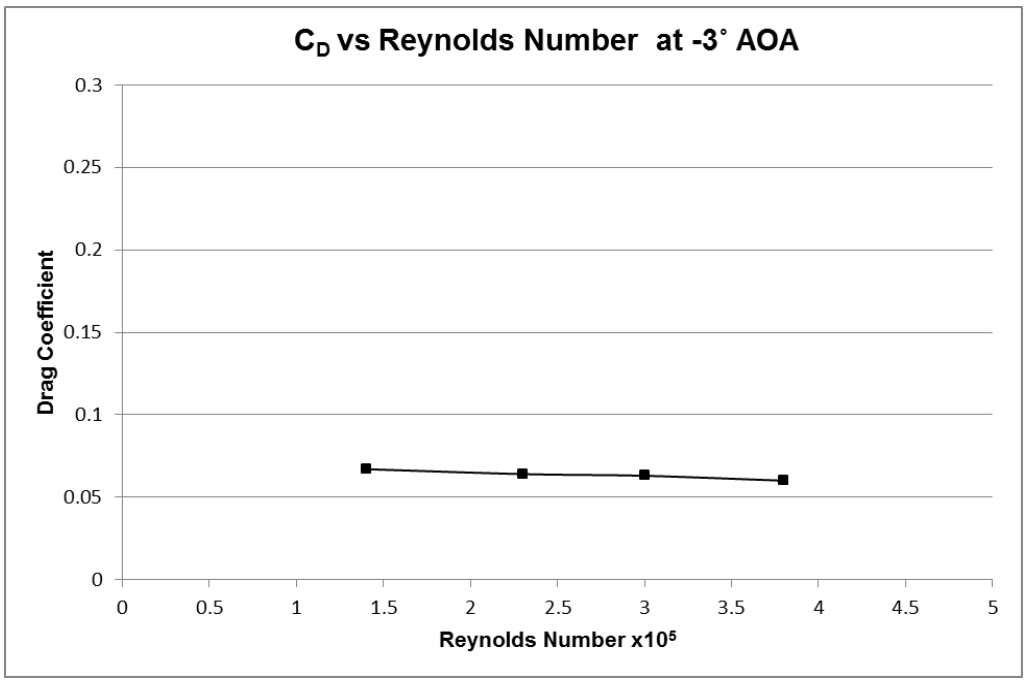

Figure 4.1: Drag Coefficient vs. Reynolds Number at -3˚ angle of attack for NACA 0015.

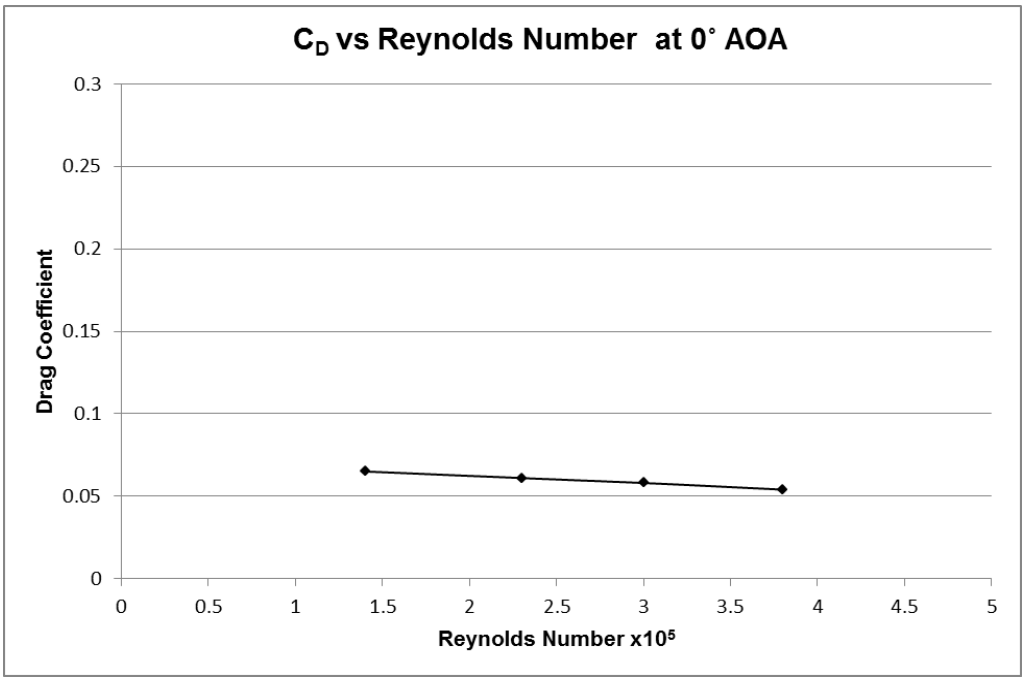

Figure 4.2: Drag Coefficient vs. Reynolds Number at 0˚ angle of attack for NACA 0015.

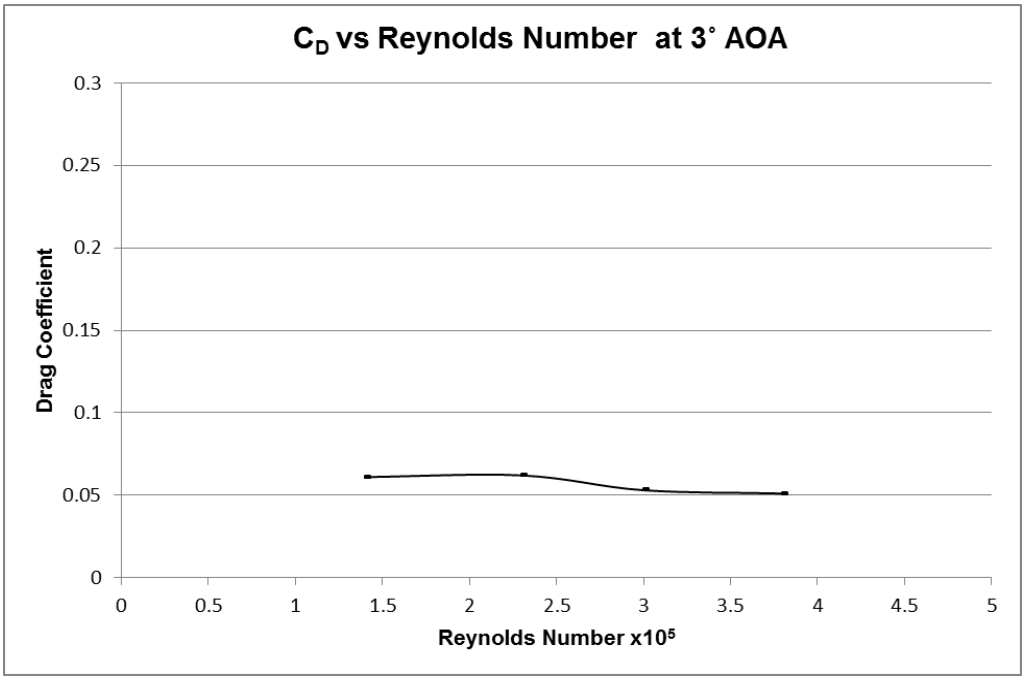

Figure 4.3: Drag Coefficient vs. Reynolds Number at 3˚ angle of attack for NACA 0015.

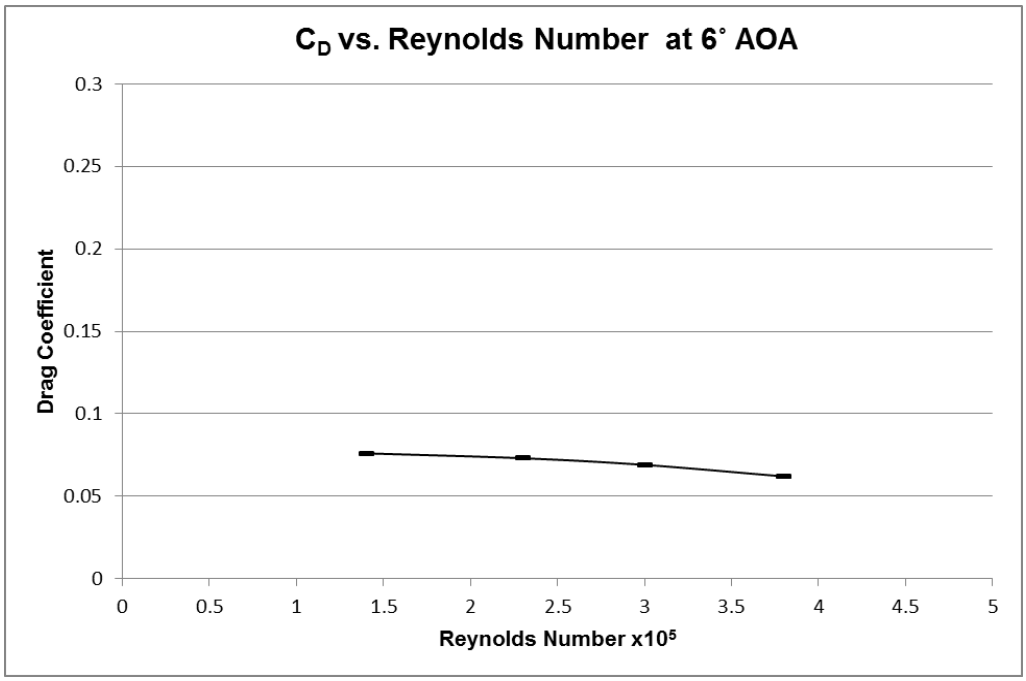

Figure 4.4: Drag Coefficient vs. Reynolds Number at 6˚ angle of attack for NACA 0015.

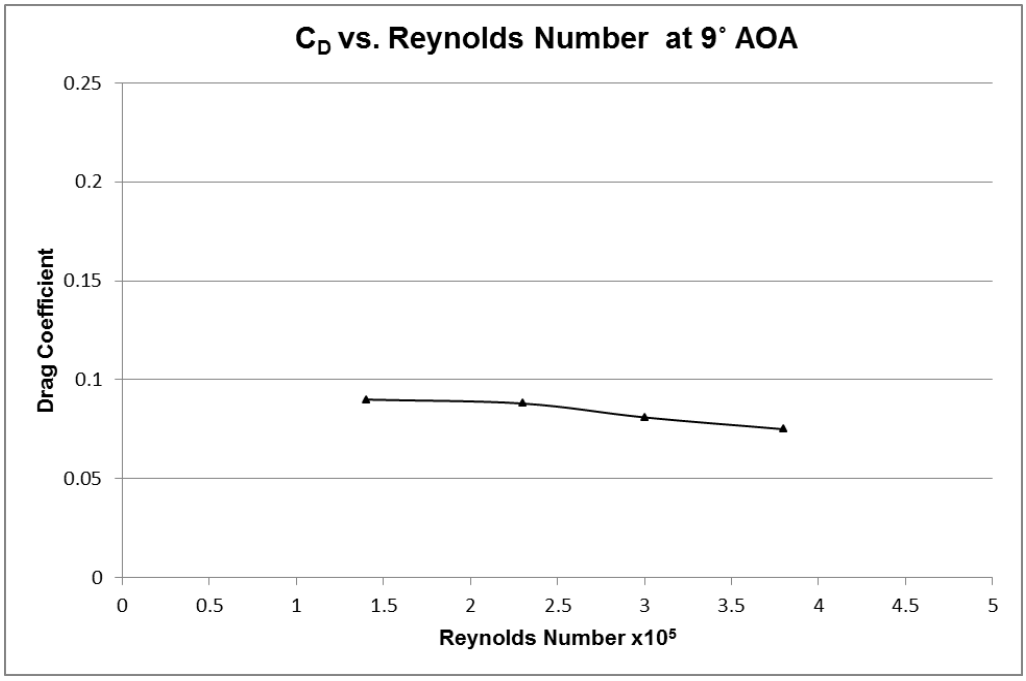

Figure 4.5: Drag Coefficient vs. Reynolds Number at 9˚ angle of attack for NACA 0015.

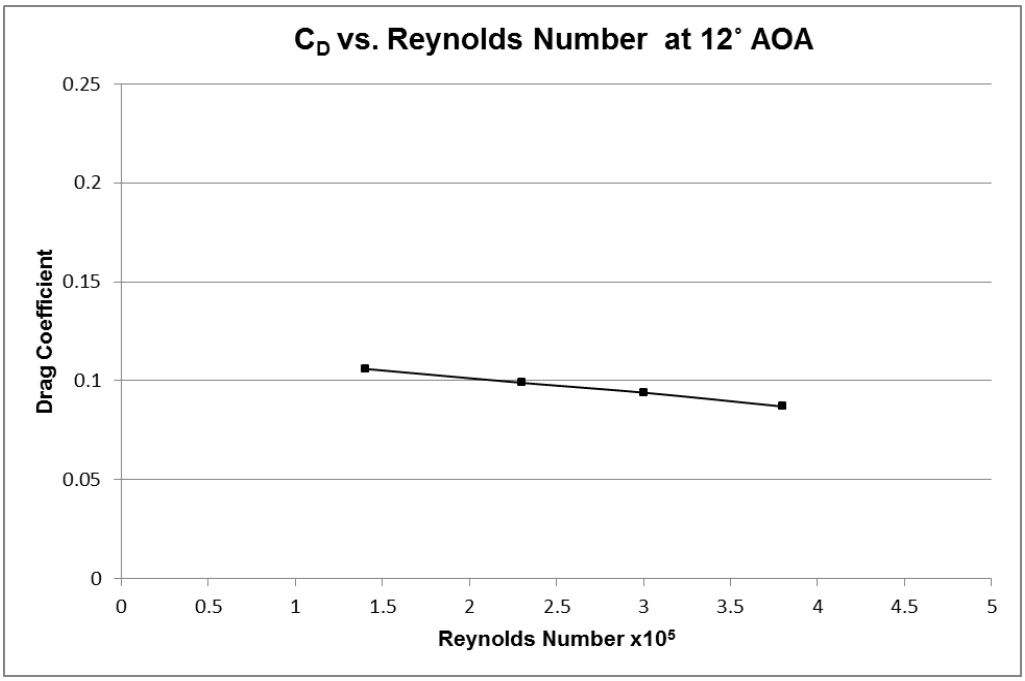

Figure 4.6: Drag Coefficient vs. Reynolds Number at 12˚ angle of attack for NACA 0015.

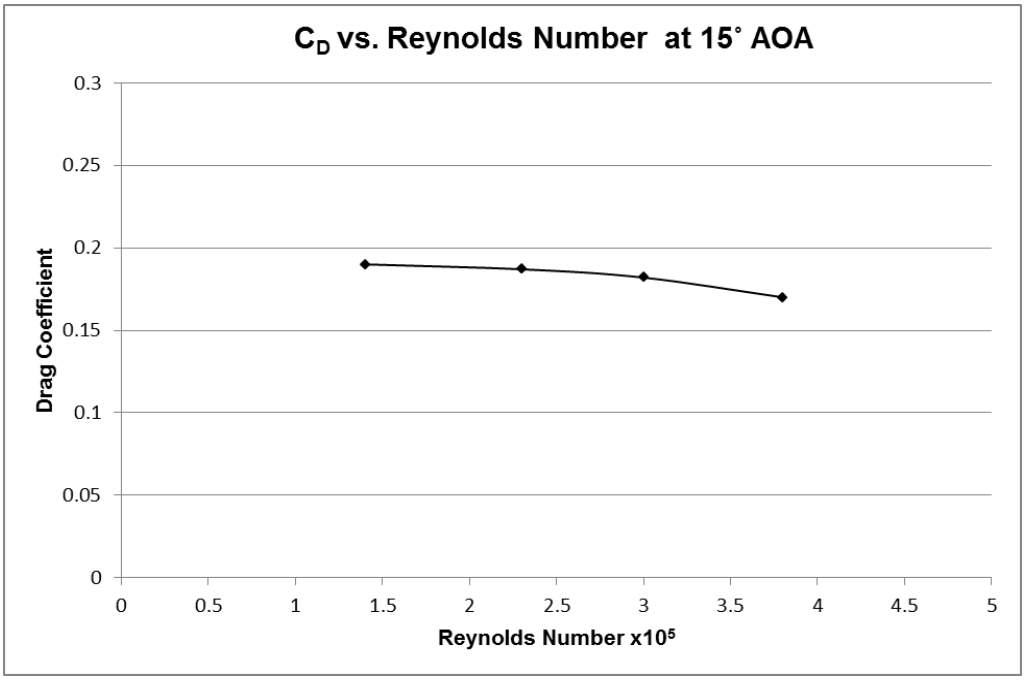

Figure 4.7: Drag Coefficient vs. Reynolds Number at 15˚ angle of attack for NACA 0015.

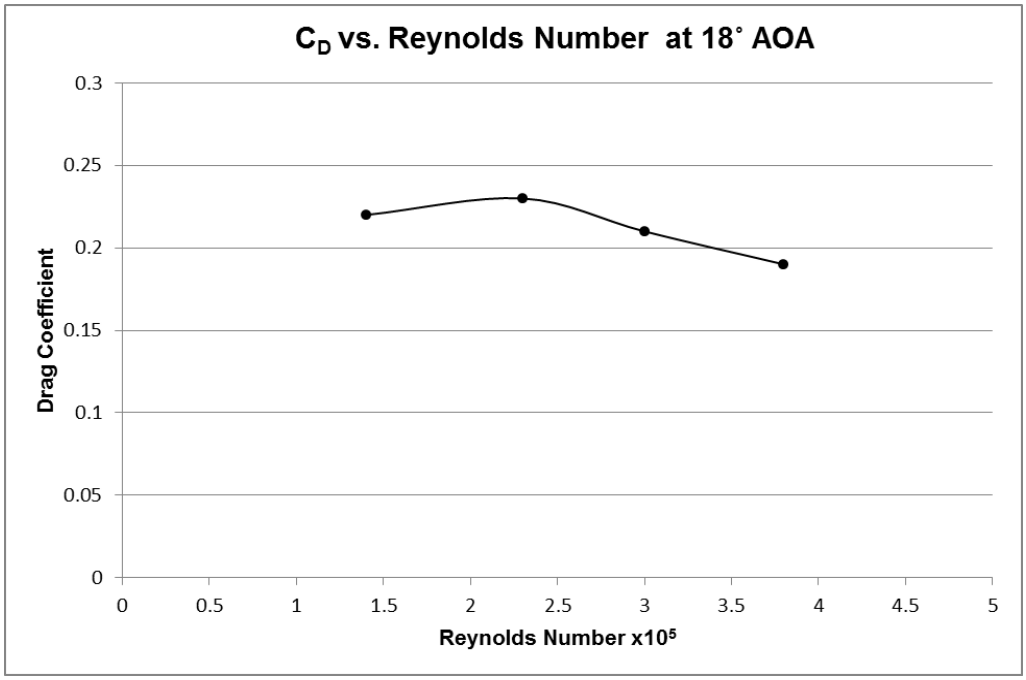

Figure 4.8: Drag Coefficient vs. Reynolds Number at 18˚ angle of attack for NACA 0015.

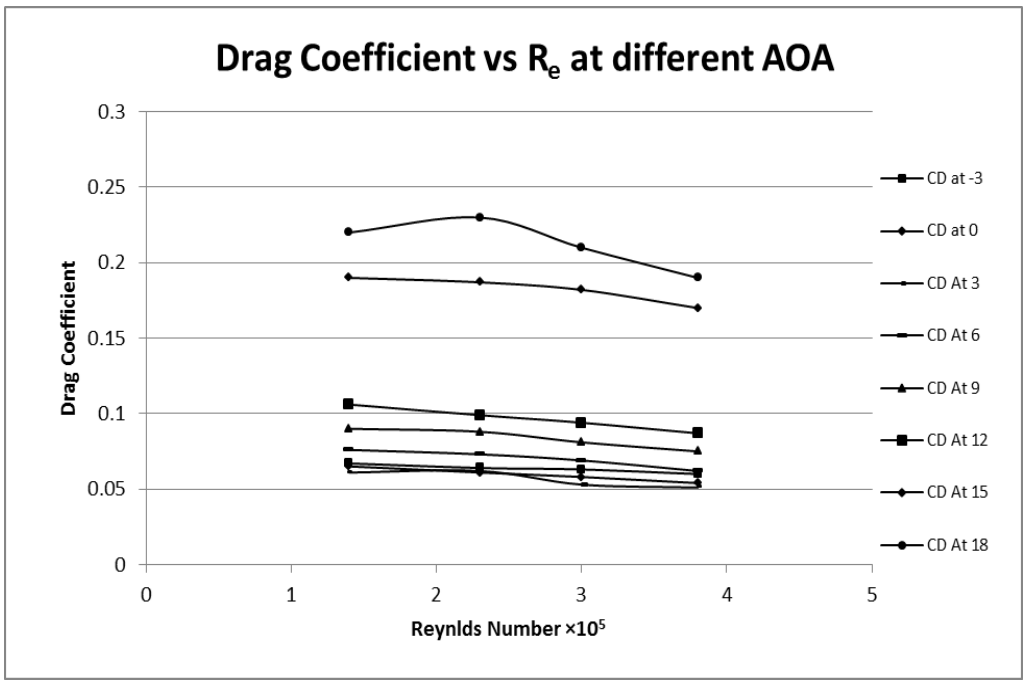

Figure 4.9: Drag Coefficient vs. Reynolds Number at different angle of attack for NACA 0015.

Now the variation of lift drag coefficient vs. angle of attack at different Reynolds number for symmetric aerofoil NACA 0015 is shown in the **Figure 4.10** and **4.11**.

The shape of the lift coefficient vs. angle of attack curve has the stall angle approximately after 14˚ AOA [7].

The shape of the drag coefficient vs. angle of attack curve is found parabolic nature. The lift and drag coefficient increase with increase of angle of attack. But with the increase of Reynolds number the lift coefficient increase and drag coefficient decreases.

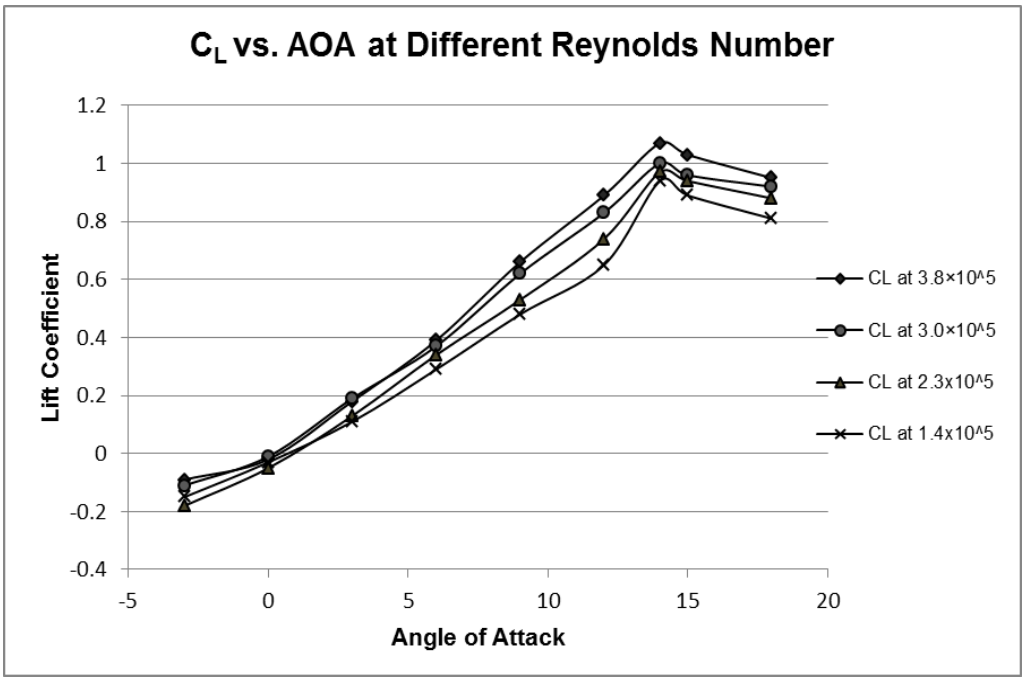

Figure 4.10: Variation of Lift coefficient vs. angle of attack at different R_e for NACA 0015.

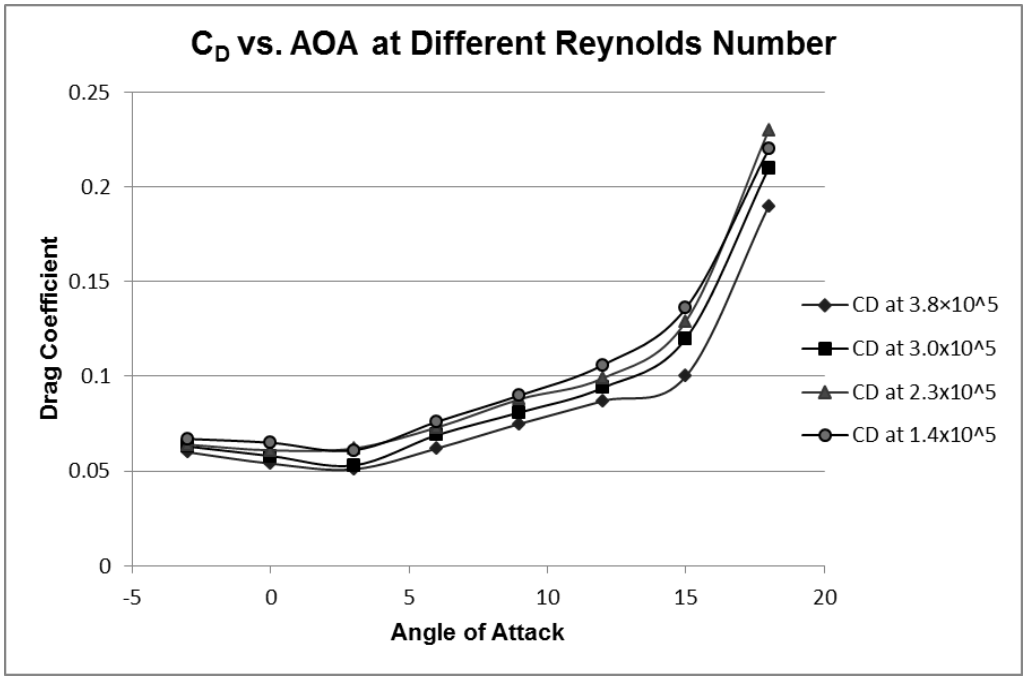

Figure 4.11: Variation of drag coefficient vs. angle of attack at different R_e for NACA 0015.

4.3 Aerodynamic Characteristics of NACA 4415

The variation of drag coefficient with Reynolds number for cambered aerofoil (NACA 4415) is shown in following **Figure 4.12** to **Figure 4.20**. The drag coefficient simultaneously decreases a little and gives downward lines with the increase of Reynolds number of the air for each angle of attack. NACA 4415 gives less drag coefficient than NACA 0015.

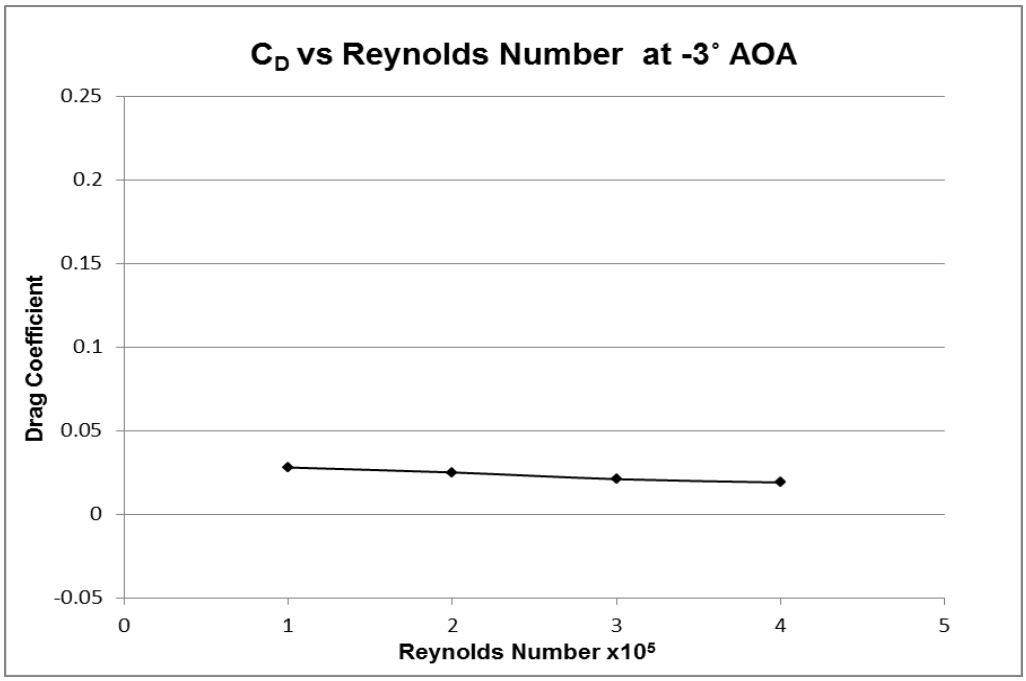

Figure 4.12: Drag Coefficient vs. Reynolds Number at -3˚ angle of attack for NACA 4415.

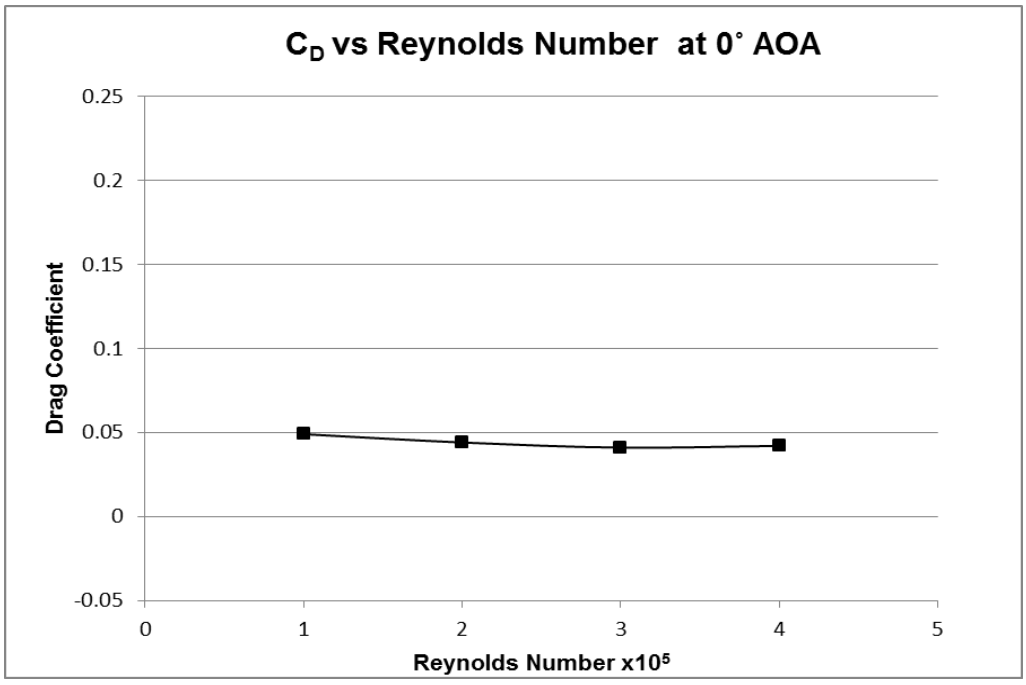

Figure 4.13: Drag Coefficient vs. Reynolds Number at 0˚ angle of attack for NACA 4415.

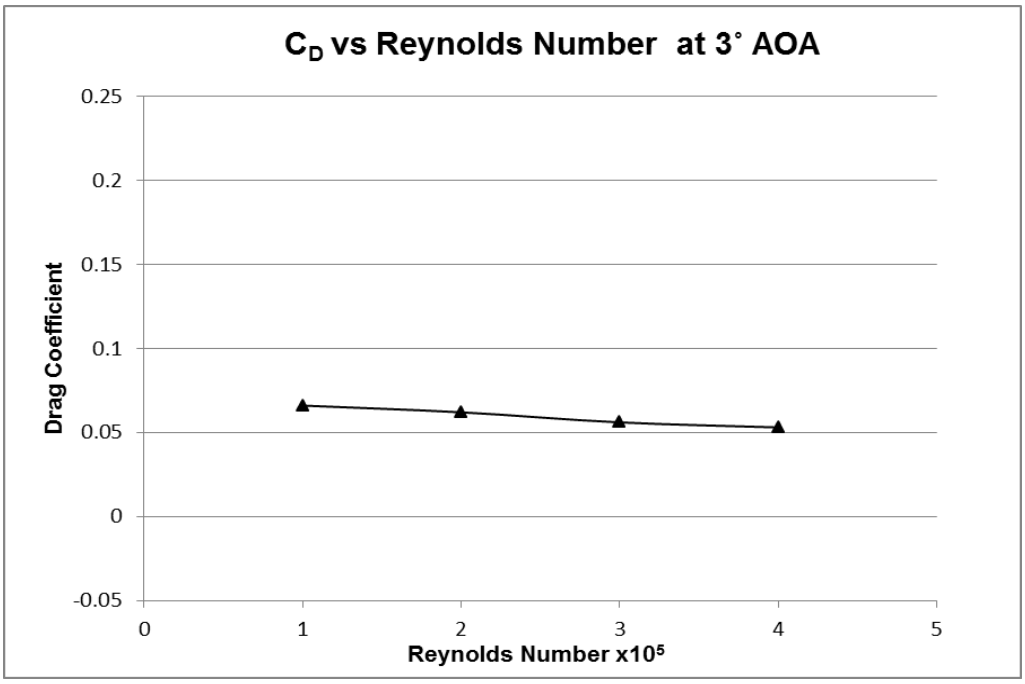

Figure 4.14: Drag Coefficient vs. Reynolds Number at 3˚ angle of attack for NACA 4415.

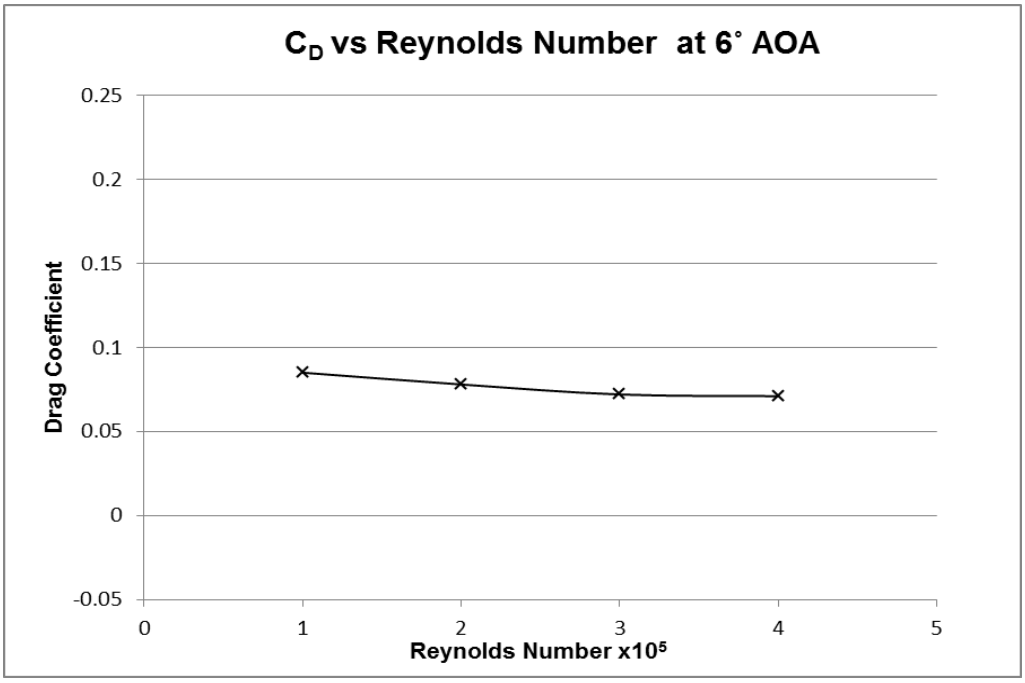

Figure 4.15: Drag Coefficient vs. Reynolds Number at 6˚ angle of attack for NACA 4415.

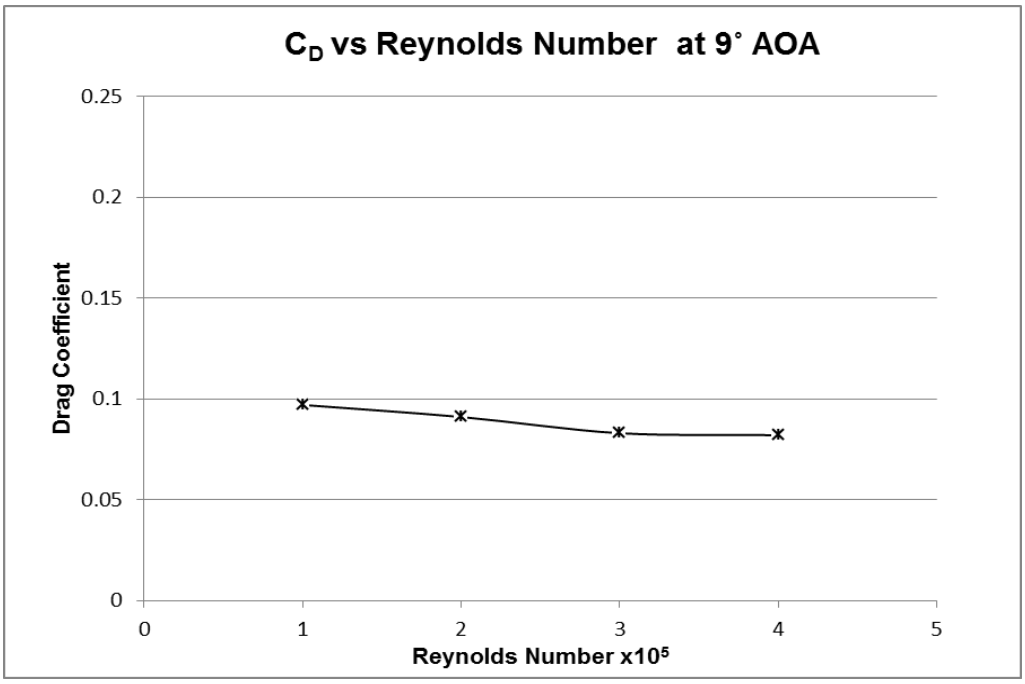

Figure 4.16: Drag Coefficient vs. Reynolds Number at 9˚ angle of attack for NACA 4415.

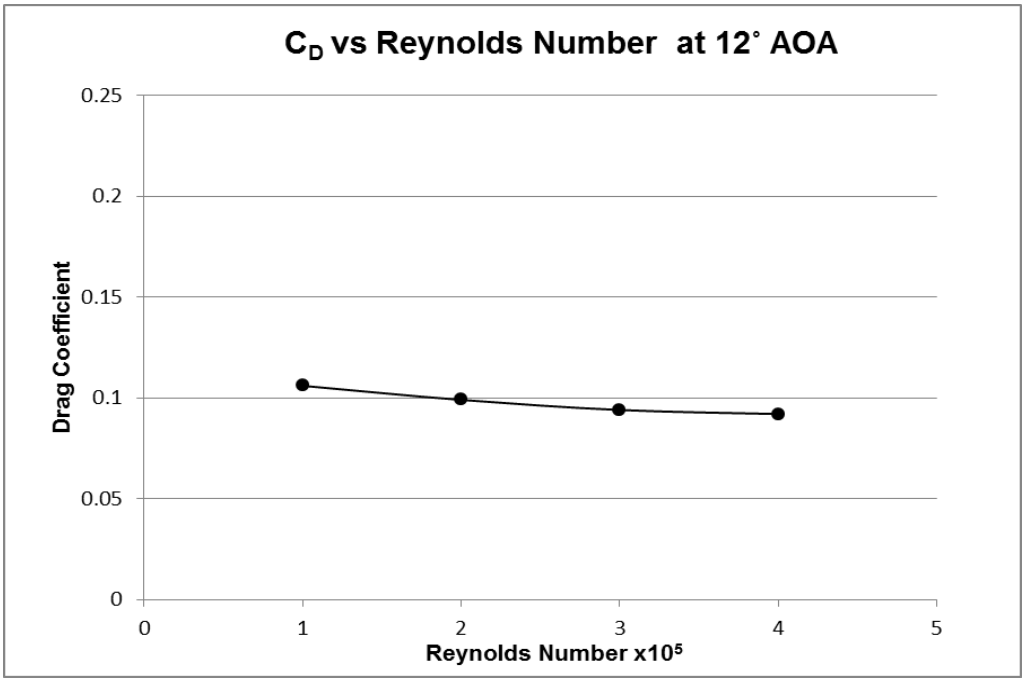

Figure 4.17: Drag Coefficient vs. Reynolds Number at 12˚ angle of attack for NACA 4415.

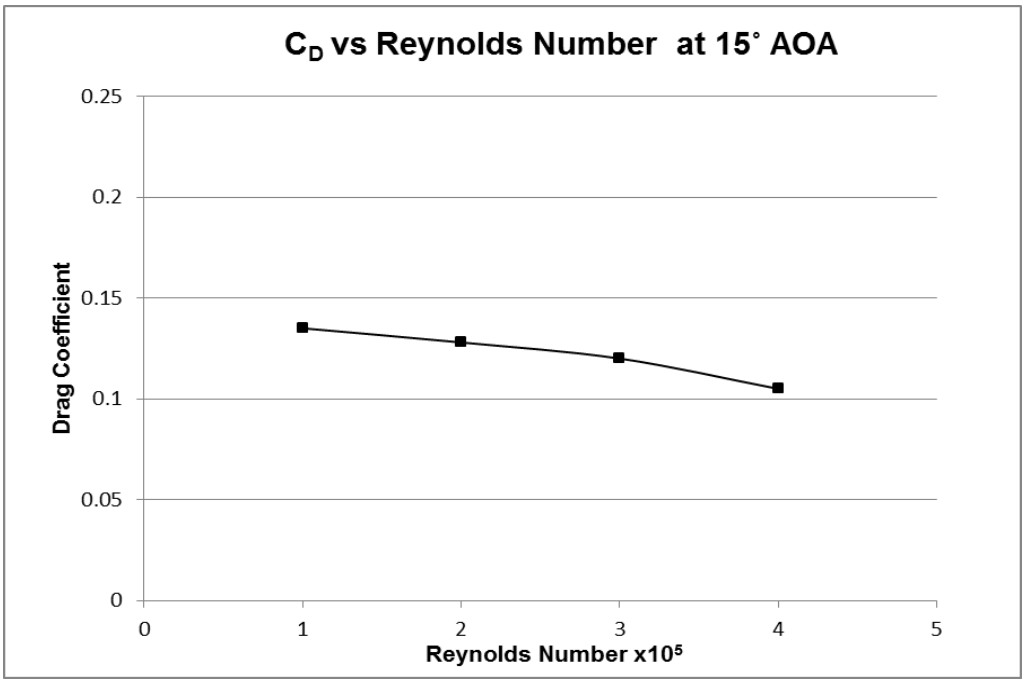

Figure 4.18: Drag Coefficient vs. Reynolds Number at 15˚ angle of attack for NACA 4415.

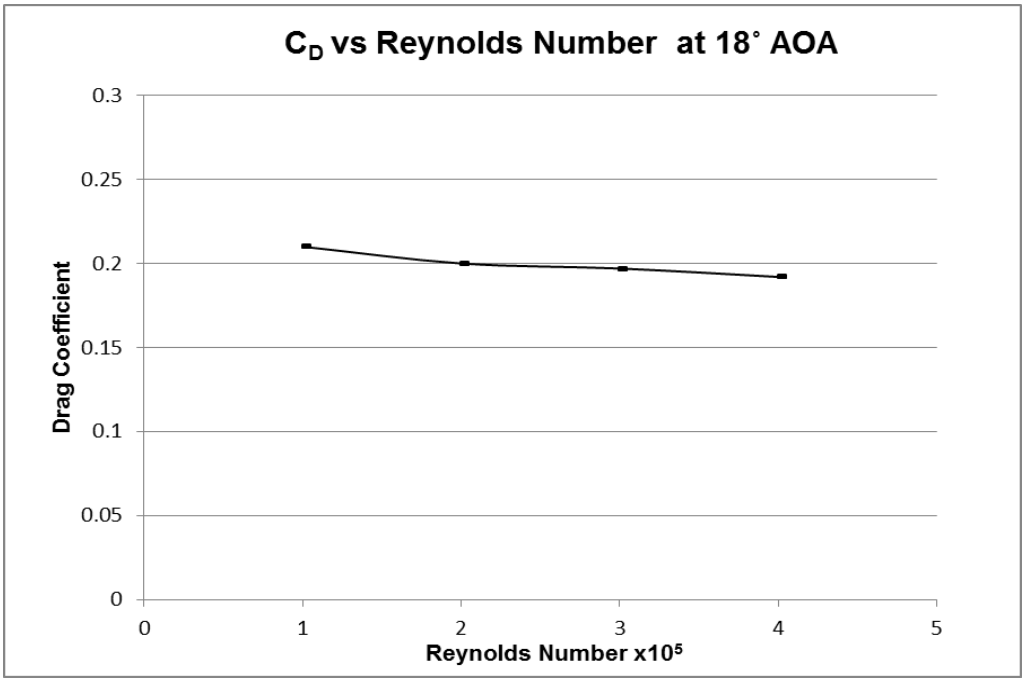

Figure 4.19: Drag Coefficient vs. Reynolds Number at 18˚ angle of attack for NACA 4415.

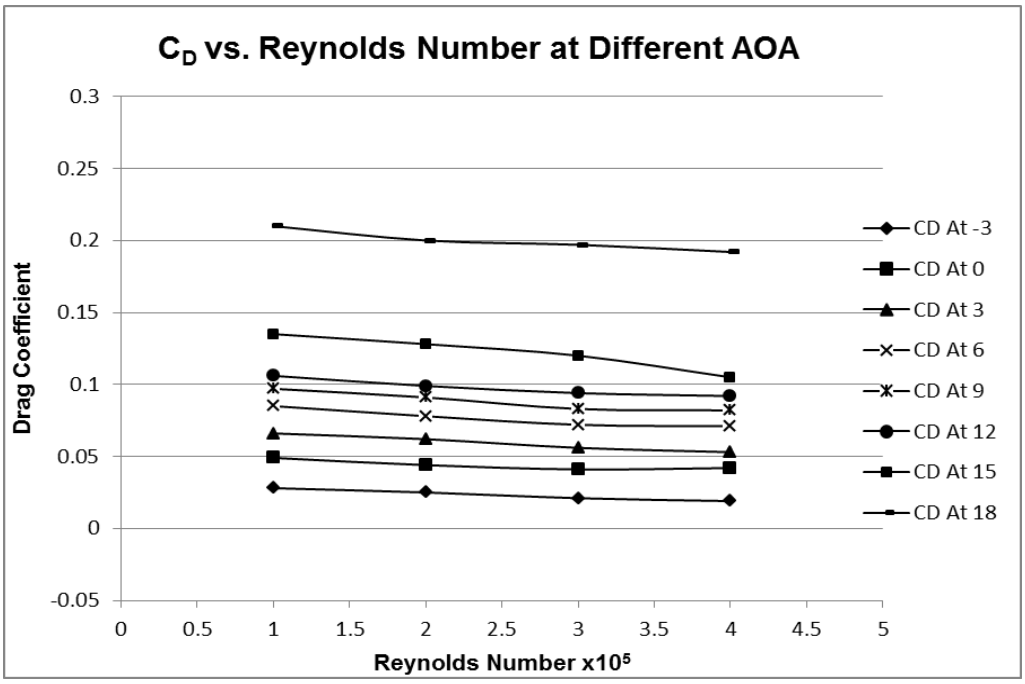

Figure 4.20: Drag Coefficient vs. Reynolds Number at different angle of attack for NACA 4415.

For symmetric aerofoil NACA 4415 the variation of lift drag coefficient vs. angle of attack at different Reynolds number is shown in the **Figure 4.21** and **4.22**. The approximate stall angle has been found after 16˚ AOA in the lift coefficient vs. angle of attack [8].

The shape of the drag coefficient vs. angle of attack curve is found parabolic nature. The lift and drag coefficient increase with increase of angle of attack. But with the increase of Reynolds number the lift coefficient increase and drag coefficient decreases.

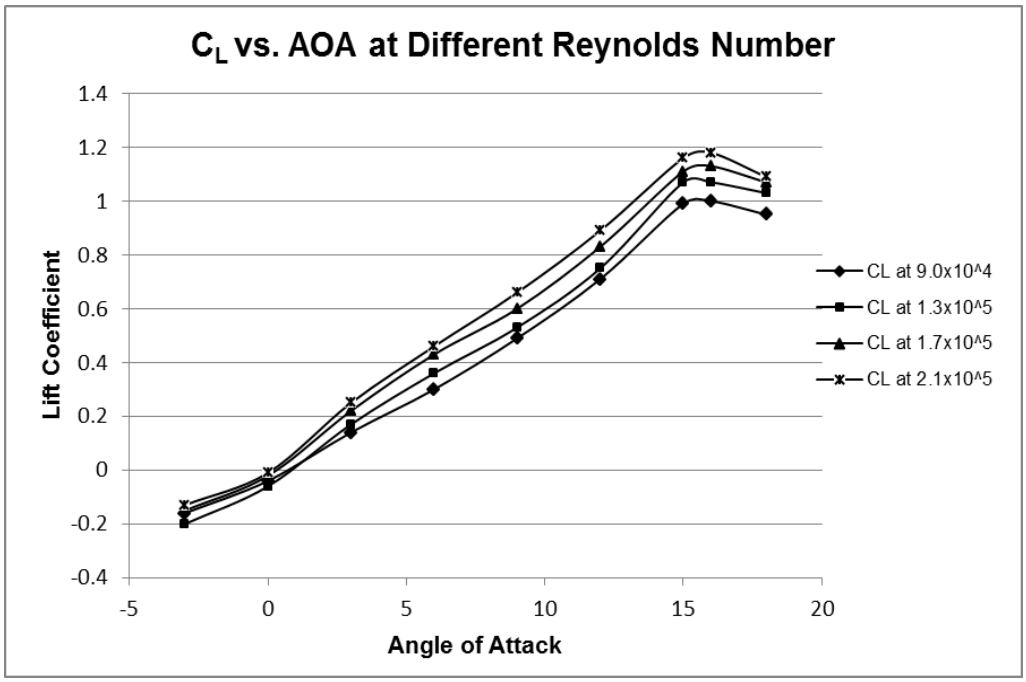

Figure 4.21: Variation of Lift coefficient vs. angle of attack at different R_e for NACA 4415.

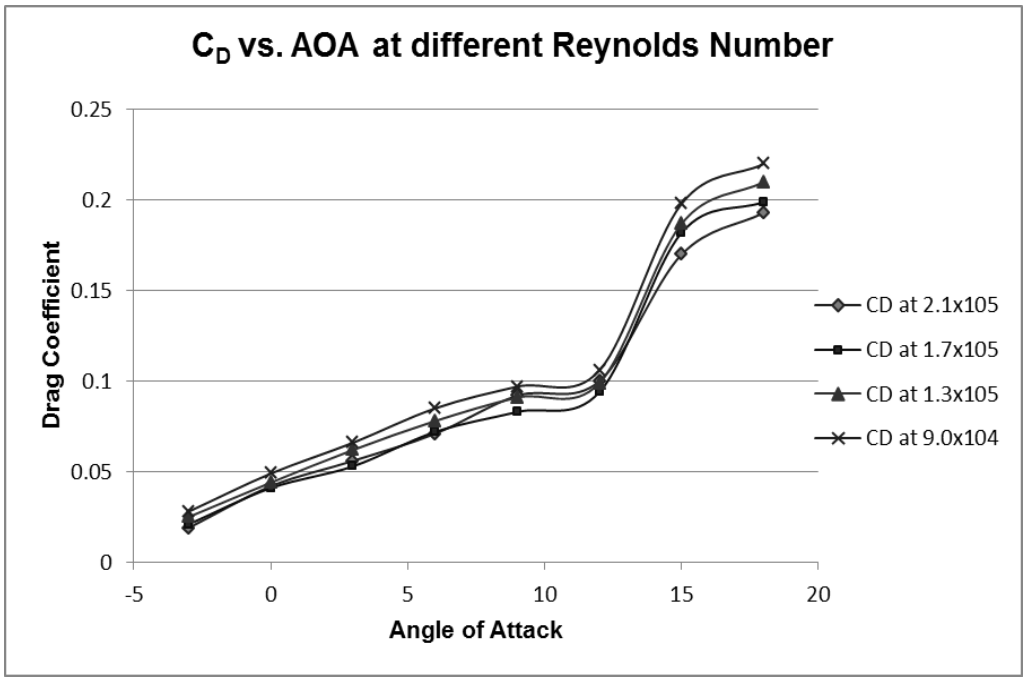

Figure 4.22: Variation of drag coefficient vs. angle of attack at different R_e for NACA 4415.

4.4 Aerodynamic Characteristics of the Cylinder

The Drag Coefficient vs. Reynolds Number curves presented in **Figure 4.23** show a significant increase in C_D with an increase in Reynolds number for cylinder. Theoretically in subsonic level of air speed the curve is a straight line in the range of Reynolds number. The ideal drag coefficient is approximately 1.2 (by Scruton and Rogers, 1971). But experimentally, the Reynolds number increases the drag coefficient gradually increases at low Reynolds number and become a straight line at high Reynolds number [4].

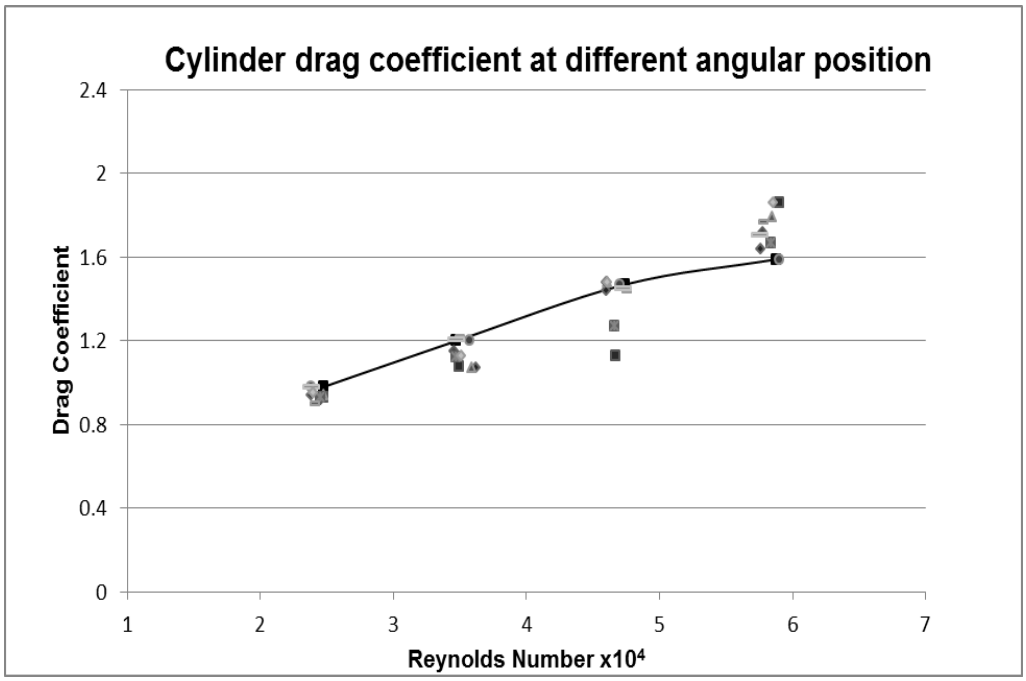

Figure 4.23: Drag Coefficient vs. Reynolds Number at different angular position for the Cylinder.

4.5 Aerodynamic Characteristics of the Sphere

Theoretically in subsonic level of air speed the curve goes downward in the range of Reynolds number. So the experimental Drag Coefficient vs. Reynolds Number for the sphere, the curves presented in **Figure 4.24** show a significant decrease in C_D with an increase in Reynolds number for all geometries though the value of Drag coefficient is much higher than the ideal values.

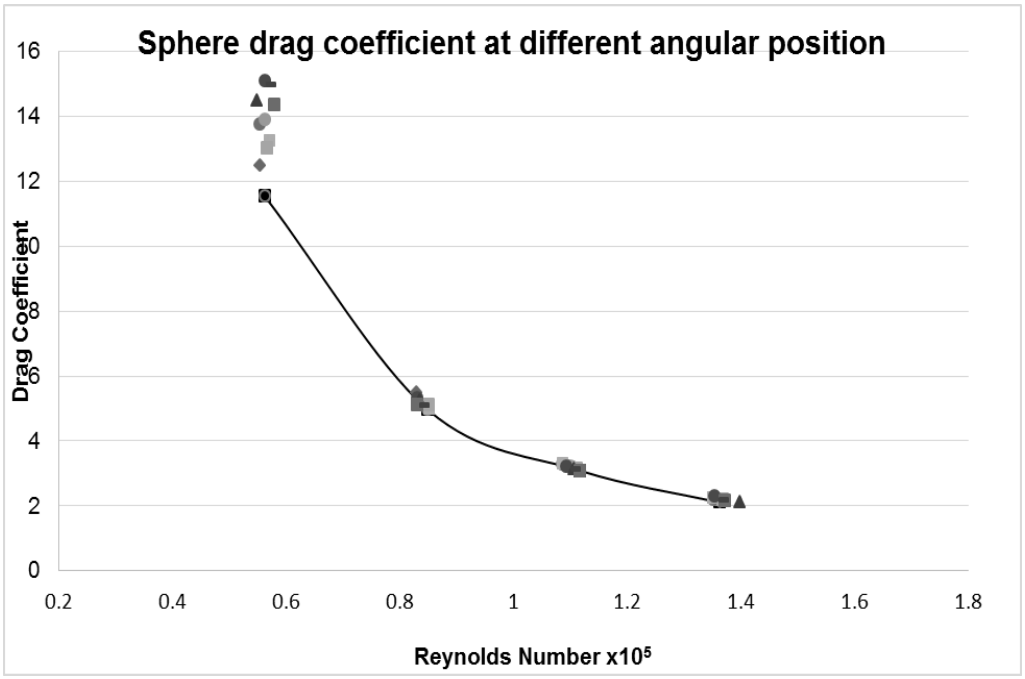

Figure 4.24: Drag Coefficient vs. Reynolds Number at different angular position for the Sphere.

CHAPTER-5

DISCUSSIONS

5.1 Comparison of Coefficient of Drag Force of Theoretical Result

The variation of coefficient of drag force with Reynolds Number for different angle of attack of NACA 0015 profile is shown in **Figure 5.1**. It is seen that the drag coefficient trends to decrease with the increase of Reynolds number. Also it is found that with increasing angle of attack the values of drag coefficient increases respectively. For example, at 0˚ AOA, $C_{D\ max}$=0.067 and at 18˚ AOA, $C_{D\ max}$=0.23.

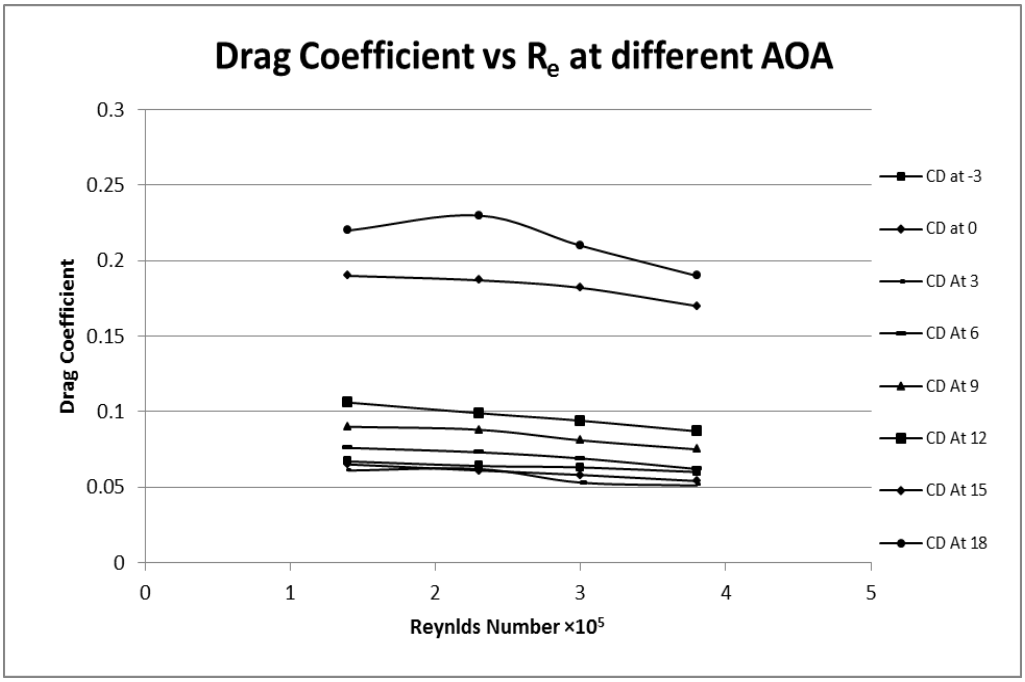

Figure 5.1: Drag Coefficient vs. Reynolds Number at different angle of attack for NACA 0015.

Similarly for cambered aerofoil NACA 4415 the variation of coefficient of drag force with Reynolds Number for different angle of attack of NACA 0015 profile is shown in **Figure 5.2**. Here the drag coefficient trends to decrease linearly with the increase of Reynolds number and at higher angle of attack.

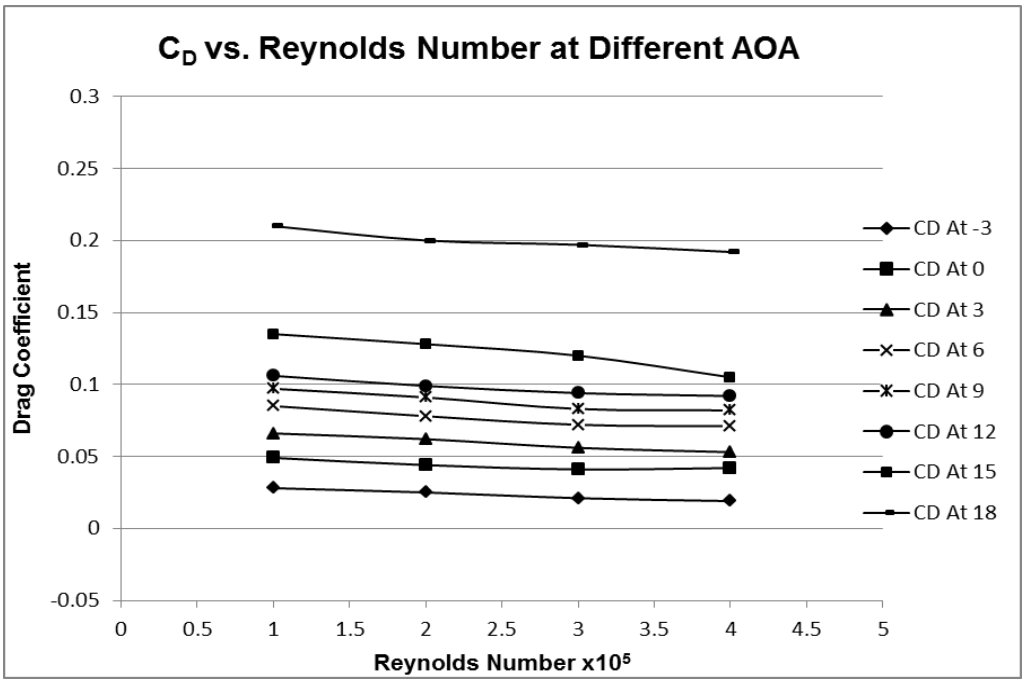

Figure 5.2: Drag Coefficient vs. Reynolds Number at different angle of attack for NACA 4415.

For the cylinder the Figure 5.3 represents the evolution of the drag coefficient according to the Reynolds number at different angular position. Theoretically in subsonic level of air speed the ideal curve is a straight line in this range of Reynolds number. The ideal drag coefficient is approximately 1.2 (Scruton and Rogers, 1971) Shown in **Figure 2.4**. But practically at low to high Reynolds number the Drag coefficient gradually rises and forms approximate constant line up to certain range of Reynolds number in the following figure [4].

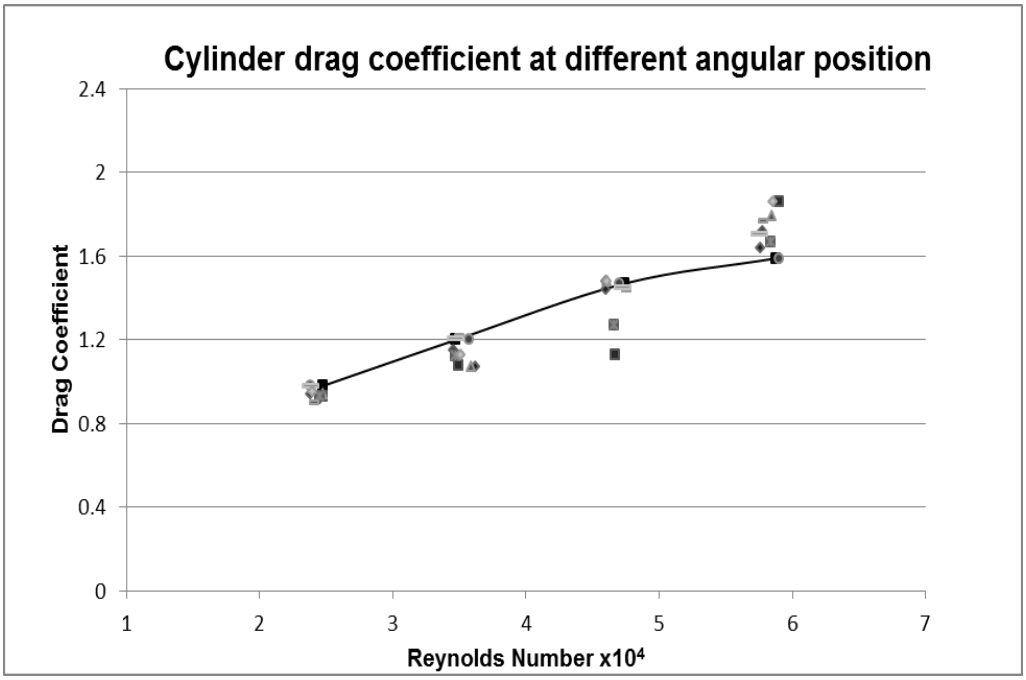

Figure 5.3: Drag Coefficient vs. Reynolds Number at different angular position for the Cylinder.

Again, theoretically the sphere in subsonic level of air speed shows a downward parabolic curve in the range of Reynolds number which has been shown in the **Figure 2.6**. The experiential drag coefficient vs. Reynolds number graph also gives a downward parabolic curve with the increase of Reynolds number. But the values of drag coefficient are much higher than the ideal values for the geometry.

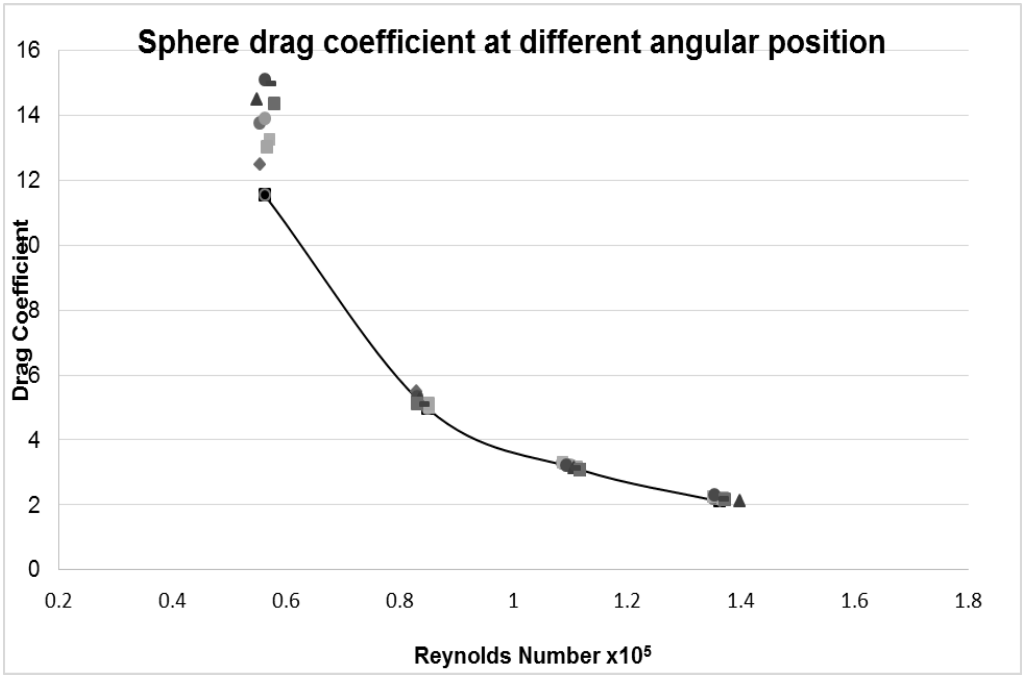

Figure 5.4: Drag Coefficient vs. Reynolds Number at different angular position for the Sphere.

The difference between the four profiles drag coefficient is quite significant. The profile which has lesser drag coefficient, the more aerodynamic shape it is. From the investigation it has been observed that the cambered aerofoil NACA 4415 have less drag coefficient than symmetric aerofoil NACA 0015. For cylinder and sphere the cylinder has less drag coefficient than the sphere [3]. And also the cylinder and sphere have much higher drag coefficient than the aerofoils. So firstly NACA 4415 and then NACA 0015 have better aerodynamic shape than the cylinder or sphere. So the Drag forces are easy to predict and control for the aerofoil than the cylinder or sphere.

Now **Table 5.1** is made based on the difference between the drag coefficients of the symmetric aerofoil NACA 0015 at 15˚ AOA, cambered aerofoil NACA 4415 at 15˚ AOA, cylinder and sphere at 10 m/s, 15 m/s, 20 m/s and 25 m/s air speed. The Table is given bellow:

Table 5.1: Comparison of drag coefficient of four profiles at different speed

Drag Coefficient of Different Profiles				
Velocity	**NACA 0015 (at stall angle)**	**NACA 4415 (at stall angle)**	**Cylinder**	**Sphere**
10 m/s	0.136	0.134	0.92	11.53
15 m/s	0.129	0.127	1.26	4.96
20 m/s	0.120	0.117	1.46	3.08
25 m/s	0.105	0.103	1.78	2.1

From the above comparisons it is clear that the cambered aerofoil is distinctly the most efficient aerodynamic shape and the sphere is the less desired aerodynamic shape which highly disturbs the air flow.

CHAPTER-6

CONCLUSIONS AND RECOMMENDATIONS

6.1 Conclusion

The main objective of this thesis is the study of drag forces of different shaped profiles in different Reynolds number. The results obtained and the graph pattern seem to agree rather well with the experimental and theoretical, in particular on the drag coefficient vs. Reynolds number curves for examined cylinders, sphere, symmetrical aerofoil (NACA 0015) and cambered aerofoil (NACA 4415). Following this investigation; it was possible to put the light on the following points:

- With the increase of Reynolds number drag coefficient decrease respectively. The change pattern varies with the profile shapes. As the drag coefficient vs. Reynolds number curve for cylinder and sphere shows parabolic shape whereas the aerofoil shows almost linier decrement od drag coefficient with the increase of Reynolds number.
- The symmetrical aerofoil (NACA 0015) and cambered aerofoil (NACA 4415) gives low drag coefficient then the cylinder and sphere, so the aerofoils are the desired aerodynamic shape where high lift forces are required like airplanes, turbine blades etc.
- Fluid flow over it essentially follows the contours of the aerofoils, so it's said to be streamlined and a body that is not streamlined is said to be bluff. The fluid flow over a bluff body follows the contours of that body only part way, or not at all, so cylinder and sphere shape are bluff.
- The drag force over a cylinder or sphere is required for the design of the vehicles, builds shapes and also fuselage of the plane.

The importance of the experimental investigation is to clear up the physical phenomena described by the theory. And it has been found that the practically the physical phenomena and theory varies a lot.

6.2 Recommendations

- The four profiles can be fabricated with even smooth surface material instead of wood to reduce surface friction drag and maintain its streamlines.

- The design and simulation of cylinder, sphere, symmetrical aerofoil (NACA 0015) and cambered aerofoil (NACA 4415) can also be done by Gambit and Fluent or other simulation software.

- In the experiment smoke can be used to visualize the streamline flow pattern of the air over the profiles.

REFERENCES

Reference Books and Links

[1] Clancy L. J.: “Aerodynamics”, John Wiley, New York, 1975.

[2] http://www.century-of-flight.net

[3] G. J. Sheard, K. Hourigan and M. C. Thompson,2004: “Computations of the drag coefficients for low-Reynolds-number flow past rings” , J. Fluid Mech. (2005), vol. 526, pp. 257–275. c 2005 Cambridge University Press

[4] A.O. Ladjedel, B.T.Yahiaoui, C.L.Adjlout and D.O.Imine: “Experimental and Numerical Studies of Drag Reduction on a Circular Cylinder”, page-359, World Academy of Science, Engineering and Technology 53 2011.

[5] http://www.grc.nasa.gov/WWW/k-12/airplane/beach.html

[6] http://www.grc.nasa.gov/WWW/k-12/airplane/dragsphere.html

[7] http://airfoiltools.com/airfoil/details?airfoil=naca0015-il#polars

[8] http://airfoiltools.com/airfoil/details?airfoil=naca4418-il#polars